Bull Volcanol (1992) 54:93-125

Bulletin of
Volcanology

Volcán Quizapu, Chilean Andes

Wes Hildreth[1] **and Robert E Drake**[2]

[1] U.S. Geological Survey, Menlo Park, CA 94025, USA
[2] Geochronology Center, Institute of Human Origins, 2453 Ridge Road, Berkeley, CA 94709, USA

Received January 10, 1991/Accepted June 4, 1991

Abstract. Quizapu is a flank vent of the basalt-to-rhyodacite Holocene stratocone, Cerro Azul, and lies at the focus of a complex Quaternary volcanic field on the Andean volcanic front. The Quizapu vent originated in 1846 when 5 km^3 of hornblende-dacite magma erupted effusively with little accompanying tephra. Between ~1907 and 1932, phreatic and strombolian activity reamed out a deep crater, from which 4 km^3 of dacite magma identical to that of 1846 fed the great plinian event of 10–11 April 1932. Although a total of >9 km^3 of magma was thus released in 86 years, there is no discernible subsidence. As the pre-plinian crater was lined by massive lavas, 1932 enlargement was limited and the total plinian deposit contains only ~0.4 wt % lithics. Areas of 5-cm and 1-cm isopachs for compacted 1932 fallout are about half of those estimated in the 1930's, yielding a revised ejecta volume of ~9.5 km^3. A strong inflection near the 10-cm isopach (downwind ~110 km) on a plot of log Thickness vs Area $^{1/2}$ reflects slow settling of fine plinian ash – not of coignimbrite ash, as the volume of pyroclastic flows was trivial (<0.01 km^3). About 17 vol.% of the fallout lies beyond the 1-cm isopach, and ~82 wt% of the ejecta are finer than 1 mm. At least 18 hours of steady plinian activity produced an exceptionally uniform fall deposit. Observed column height (27–30 km) and average mass eruption rate (1.5×10^8 kg/s) compare well with values for height and peak intensity calculated from published eruption models. The progressive "aeolian fractionation" of downwind ash (for which Quizapu is widely cited) is complicated by the large compositional range of 1932 juvenile pumice (52–70% SiO_2). The eruption began with andesitic scoria and ended with basaltic scoria, but >95% of the ejecta are dacitic pumice (67–68% SiO_2); minor andesitic scoria and frothier rhyodacite pumice (70% SiO_2) accompanied the dominant dacite. Phenocrysts (pl > hb ~ opx > mt > ilm ~ cpx) are similar in both abundance and composition in the 1846 (effusive) and 1932 (plinian) dacites. Despite the contrast in mode of eruption, bulk compositions are also indistinguishable. The only difference so far identified is a lower range of δD values for 1846 hornblende, consistent with pre-eruptive degassing of the effusive batch.

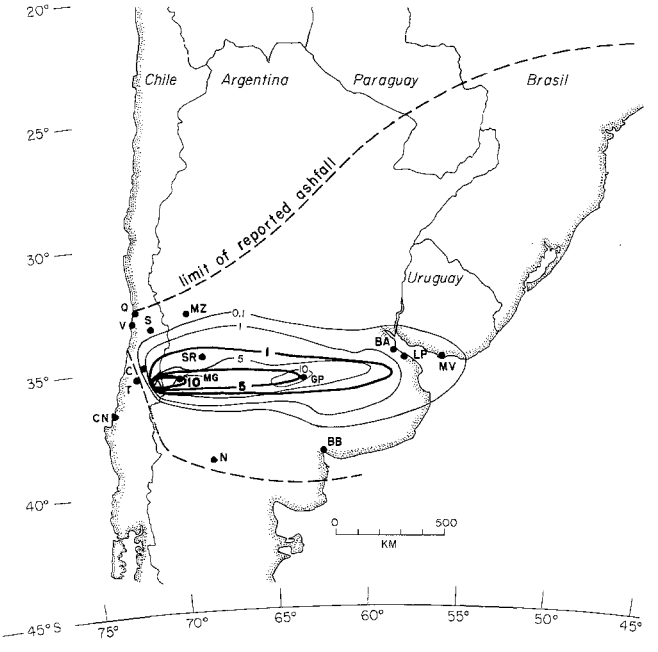

Fig. 1. Location map and regional isopachs for compacted 1932 Quizapu fallout; thickness in cm. *Fine lines* are from Larsson (1937), based on a compilation of uncompacted thicknesses reported principally by Argentine railway companies; *bold isopachs* are based on our measurements made in 1980–1991. For proximal isopach data, see Fig. 8. Cities and towns: *BA* Buenos Aires; *BB* Bahía Blanca; *C* Curicó; *CN* Concepción; *GP* General Pico; *LP* La Plata; *MG* Malargüe; *MV* Montevideo; *MZ* Mendoza; *N* Neuquén; *Q* Quintero; *S* Santiago; *SR* San Rafael; *T* Talca; *V* Valparaíso. The border between Chile and Argentina is the Andean crest and continental divide, lying ~30 km east of the Quizapu vent

Offprint requests to: W Hildreth

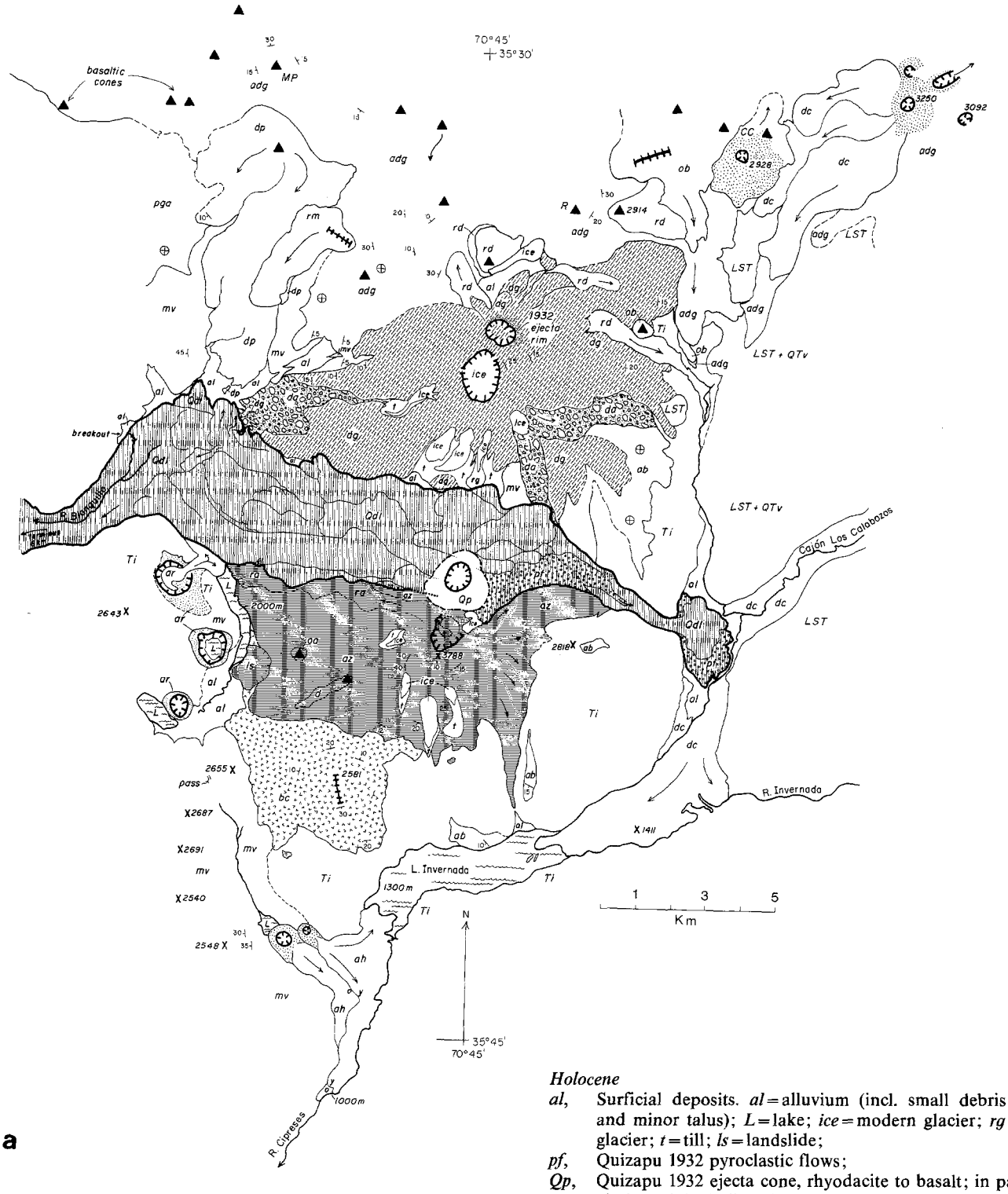

a

Holocene

al, Surficial deposits. *al* = alluvium (incl. small debris flows and minor talus); *L* = lake; *ice* = modern glacier; *rg* = rock glacier; *t* = till; *ls* = landslide;

pf, Quizapu 1932 pyroclastic flows;

Qp, Quizapu 1932 ejecta cone, rhyodacite to basalt; in part agglutinated, including sheet on N slope of Cerro Azul;

Qdl, Quizapu 1846–47 dacite lava flows;

ra, rhyodacite lava and agglutinate of Cerro Azul;

ar, mafic lava and ejecta of the three La Resolana craters;

ah, andesite lava and ejecta of Los Hornitos (*y* = younger, *o* = older);

rm, rhyodacite lava of Alto de Las Mulas;

da, debris-avalanche deposits of Volcán Descabezado Grande;

az, basaltic and andesitic lavas and ejecta of Cerro Azul (*oa* = flank cone of olivine andesite; *d* = flank flow of dacite);

dc, postglacial andesite-dacite lavas and ejecta (*stipple*) of Volcán Descabezado Chico;

Fig. 2. a Geologic map of Quizapu and the Azul-Descabezado cluster. Based on fieldwork in 1980, 1982, 1984, 1985, 1988, and 1991. Lava flows of 1846–47 flowed both east and west from the Quizapu vent on the drainage divide. Several meters of 1932 pumiceous fallout covers most of the map area. Craters are indicated by *hachures*, fissure vent by a *trellis*, and other vents by *triangles* (▲). Elevations are given in meters. **b** Location map showing topography and place names. Base from Río Claro and Volcán Descabezado Chico 1:50000 sheets, 1978 editions, Instituto Geográfico Militar de Chile. Explanation of **a**:

b

Holocene and/or latest Pleistocene

- *dg*, dacite and andesite lavas and ejecta of Volcán Descabezado Grande;
- *rd*, rhyodacite lavas north and east of Volcán Descabezado Grande;
- *dp*, aphyric dacite lava of Cerro La Palizada;
- *ob*, olivine basalt west and south of Cerro Colorado;

Late Pleistocene

- *cc*, mafic ejecta (*stipple*) and lavas of Cerro Colorado;
- *adg*, glaciated andesite and dacite lavas of recognized centers, principally Cerro Manantial Pelado, Cerro Rajaduras, and Volcán Descabezado Chico (all at N edge of map);
- *LST*, Loma Seca Tuff (0.15-Ma and 0.3-Ma regional ignimbrites);
- *ab*, andesitic lavas of Estero Barroso (0.33 Ma);
- *bc*, basalt of Las Casitas (0.34 Ma);

Pre-glacial Basement Rocks

- *pga*, extensive stacks of subhorizontal andesitic lavas from unidentified vents (1.1 Ma at Cordón El Despalmado);
- *QTv*, undifferentiated late Cenozoic pyroclastic rocks and lavas (cf. Campanario Formation of Drake 1976);
- *Ti*, Invernada pluton (7 Ma): granodiorite, tonalite, diorite, minor granite;
- *mv*, Deformed and altered, intermediate and silicic volcanic rocks with metasedimentary rocks intercalated locally. Thought to be Late Cretaceous in age

Introduction

Volcán Quizapu (pronounced kee-SAH-poo), a flank vent of the stratocone Cerro Azul, has produced the two most voluminous historic eruptions in South America. Although each eruption released 4–5 km^3 of compositionally similar dacite magma, the event of 1846–47 was largely effusive while that of 1932 was entirely pyroclastic. Plinian dispersal of the 1932 fallout across the continent (Fig. 1), the wide compositional range (52–70% SiO_2) of the 1932 ejecta, the unusually large volumes, and the contrasting styles of eruptions only 86 years apart are features that make Quizapu especially worthy of study. Moreover, the focal position of the Quizapu vent within a complex volcanic system (Fig. 2) having no fewer than 12 Holocene vents and eruptive products ranging from basalt to rhyolite (51–72% SiO_2) suggested that a broader investigation of the system as a whole might provide insights concerning subvolcanic plumbing and processes of magmatic evolution.

Quizapu itself is a small but complex constructional edifice (Fig. 3) surrounding a deep crater (Fig. 4), situated at 3000 m elevation in the pass between two stratocones, at 35°38′S in a roadless part of the Andes called the Cordillera de Talca. The crater lies ~50km east of the Chilean Central Valley and ~30 km west of the Argentine border, access being by foot or horseback over 20–40 km of rugged terrain from the villages of Radal, Vilches, or Cipreses.

The Azul-Descabezado Volcanic Cluster

Cerro Azul (3788 m) and Volcán Descabezado Grande (3953 m) are adjacent stratocones, each with ~1500 m relief, standing only 7 km apart summit-to-summit and dominating a 20 × 30-km late Quaternary volcanic field (Fig. 2) on the volcanic front of the Andean Southern Volcanic Zone. The two main edifices are largely of early Holocene and latest Pleistocene construction. Although both cones are sculpted and locally oversteepened by small Neoglacial cirques, they clearly postdate the Pleistocene ice that carved 500-m-deep gorges into the Pleistocene and older rocks that underlie them. These include an extensive 7-Ma granodioritic pluton as well as undeformed stacks of andesitic lavas, for which K-Ar dating has yielded ages of 0.3 Ma at the east base of Descabezado Grande and 1.1 Ma several km NW of it (Drake 1976; Hildreth et al. 1984). Young lavas of Cerro Azul lap SW onto a glacially eroded basaltic shield, deeply incised by Cajón Las Casitas (Fig. 2), that we have dated at 0.34 Ma (Drake, unpubl). In addition to our own work just cited, previous reconnaissance studies in the area include those of Domeyko (1903), Fuenzalida (1941, 1942, 1943), Godoy (1984) and González and Vergara (1962).

Descabezado Grande is a stout flat-topped cone that has a basal diameter of ~11 km, a volume of ~30 km^3, and a 1.4-km-wide ice-filled summit crater. The volcano consists predominantly of andesite-to-rhyodacite ejecta, agglutinate, and fountain-fed lava flows. Cerro Azul is a steep slender cone only ~11 km^3 in volume, having a 500-m-wide asymmetrical crater, which is open to the northeast and deeply mantled by 1932 ejecta. Azul also consists largely of agglutinated pyroclastics and derivative lavas, although a few andesitic and dacitic lava flows vented effusively on the lower flanks. Its summit-derived agglutinate sheets span the extraordinary range of 51–69% SiO_2, which is almost identical to the range for 1932 ejecta from Azul's most productive flank vent, Quizapu.

In addition to Quizapu and the stratocone pair, the volcanic field (Fig. 2) includes the following young centers: (a) five monogenetic mafic-scoria vents (units ah, ar) along the SW periphery, all Holocene in age; (b) seven separate rhyodacite lava flows (rd, rm) at the north base of Descabezado Grande, all late Pleistocene and Holocene in age; an eighth such flow (also Holocene) dams the Rio Lontué ~13 km north of the stratocone (slightly north of Fig. 2); and (c) a group of late Pleistocene mafic-scoria cones (Cerro Colorado) a few km NE of Descabezado Grande, where the field merges northeastward into other long-lived clusters of vents called Volcán Descabezado Chico and Cerro del Medio (Hildreth et al. 1984). About 15 more late Quaternary andesitic and basaltic centers along the north fringe of Figure 2, including the large, glacially dissected, edifices of Cerro Manantial Pelado and Cerro Rajaduras, are considered integral parts of the volcanic field, but they have not yet been mapped in detail. The geological and geochemical evolution of the field as a whole is under continuing investigation.

Although the main cones are plainly visible from many towns in the Chilean Central Valley, where European settlement began in the 16th century, neither eruptive nor fumarolic activity had ever been reported in the Azul-Descabezado cluster prior to 1846.

Eruptions of Quizapu

Eruption of 1846

The sketchy eruption narrative that follows owes principally to oral reports by arrieros (backcountry herdsmen), as recounted by Domeyko (1903) and Fuenzalida (1943), and also to Domeyko's own field observations made in 1849 (26 months after the outbreak), 1857, and 1873. Although a major trans-Andean livestock trail traversed the pass (Portezuelo del Viento) between the stratocones, there is neither narrative nor field evidence that any kind of vent or fumarole existed at the site of Quizapu prior to the outbreak of 26 November 1846. No precursory phenomena were reported. An arriero who had stopped to camp on the canyon floor ~7 km east of the site reported that the eruption began abruptly in the late afternoon with a great noise and a cloud of ash but without earthquakes. His companion had ridden westward through the pass a few hours earlier (about midday), within 1 km of the eruption site, noticing nothing unusual.

Fig. 3. Quizapu cone on the north flank of Cerro Azul (3788 m), viewed southwestward from near hill 2888 (5 km NE). A late coulee of 1846–47 dacite, ~1.5 km wide and ~200 m thick, sprawls into the upper basin of Quebrada Azul. The cone has 150–250 m local relief; its outer slopes are mantled with 1932 basaltic and andesitic scoria. The 1932 dacite pumice fall is >5 m thick in the foreground; on the slopes of Cerro Azul above and behind the crater, it is thicker still, agglutinated, and fissured by downslope creep

Fig. 4. Quizapu crater on the north flank of Cerro Azul, viewed southward from the summit of Descabezado Grande. Crater rim is 700 m in diameter. Far (south) rim is at 3200 m elevation, summit of Azul at 3788 m, and Portezuelo del Viento in foreground at 2800 m. Lavas in foreground are proximal coulees of 1846–47 dacite up to 200 m thick, mantled by several meters of 1932 fallout (and snow). Black scoria drapes the north and east sides of the crater

Phenomena reported that night include a continuous roar punctuated by sounds like shots, a clattering sound like that of great rockslides (probably block lavas), thunder and lightning, many blue flames, and intolerable sulfurous fumes. Although the two arrieros spent the night within 10 km of the eruption site, on opposite flanks, there was no mention of earthquakes or ashfall.

Beginning in the late afternoon and lasting throughout the next day, eruption noises were audible in the Central Valley at least as far as Talca (85 km WNW). Valley residents also reported severe rainfall, sulfurous

odors that reached them during the second day, and at night a fiery glow (lightning only?) reflecting intermittently from clouds over the Cordillera. Just as in the mountains, however, no earthquakes were felt and little or no ashfall took place (cf. Domeyko 1903, p. 423; Fuenzalida 1943, p. 44). On the third day (28 November), the eruption as witnessed from afar is said to have quieted down.

When arrieros first attempted to recross the pass about 15 days later, they found it obstructed by blocky lavas emitting abundant fumes and "small flames" (llamitas). After detouring clockwise around Descabezado Grande, they discovered that the easterly tongue (Fig. 2) of fuming lavas had already overrun the lowland meadows (Vegas de San Juan) 1400 m lower and ~7 km east of the vent. Emplacement of the larger westerly flow complex seems to have taken much longer, however, as these arrieros reported that the lava was still far from reaching their pastures along the Rio Blanquillo. Moreover, when Domeyko traversed the whole lava field in January 1849, he estimated its east-west width to be 8 or 9 km, whereas it is today more than twice that (Fig. 2) – not even including the additional 8-km-long intracanyon tongue down the Blanquillo. Domeyko expressed skepticism, but the arrieros told him during his second visit (February 1857) that the lavas had continued to advance westward, possibly as late as 1853–54 (Domeyko 1903, p. 434).

Although he didn't recognize the effusive nature of the blocky dacitic lava flows that he first visited in January 1849, Domeyko commented on their extreme cragginess, their extensive levees, and the step-like terrain resulting from many superimposed flow lobes. Not merely near the vent but virtually all over the extensive surface of the still-hot flows, he observed rapid snowmelt, phreatic explosions, multi-colored sublimates, and countless steam plumes and acid fumaroles. When he next returned in February 1857, the lavas were still fuming extensively, but there were no more phreatic outbursts or other noises from the flows; the arrieros told him that the volcano had been silent for 3 years. On his third and final expedition in February 1873, Domeyko found no surviving fumaroles and was told by the arrieros that the last had died out 4 or 5 years before. He saw no change in configuration of the lava field nor of the adjacent stratocones, and he repeatedly emphasized the absence of ash and pumice deposits and the lack of any kind of crater. Domeyko's descriptions (1903, p. 429–430) and those of Vogel (1920) suggest, however, that a fissure vent may have extended from the site of the present crater northward a few hundred meters toward the pass (Fig. 2b).

The 1846–47 lavas evidently covered any initial near-vent ejecta, and their prolonged extrusion (lasting for months and perhaps years) was accompanied by only trivial production of tephra. In common with a few prehistoric (Holocene) dacite and andesite lavas from peripheral vents along the north and west flanks of Cerro Azul (Fig. 2), the 1846 eruption neither excavated a crater nor constructed a cone. Although occupying the same position as at least part of the 1846 vent, the cratered cone now known as Quizapu is a 20th-century creation.

Precursory activity 1907–1932

As Cerro Azul and Descabezado Grande are widely visible from towns and farms in the Central Valley, the lack of any report of further activity for several decades (Bruggen 1950) probably reflects a real period of quiescence. Beginning in about 1907, however, white vapor plumes and small ashclouds were frequently seen above Quizapu (Vogel 1913); at least a few of these were explosively generated, and one of the most vigorous (on 8 September 1914) is said to have risen to a height of 6–7 km in about 8 minutes (Fuenzalida 1943). Without elaboration, Bruggen (1950) reported that Quizapu's crater had originated in 1910, but Vogel (1913) reported explosive activity in July 1907 and perhaps as early as January 1903. A photograph taken from ~8 km NW in 1916 (Riso Patrón 1917; Reck 1933) shows the profiles of the Cerro Azul and Quizapu cones much as they are today. The configuration of the crater, its fumaroles, and some of its sporadic (phreatic?) explosions were described by Vogel (1913, 1920), who visited the area in 1912, 1913, and 1916.

From 1916 to 1926 the explosions and plumes seen from the Central Valley grew more violent and increasingly frequent, sometimes occurring on a daily basis. Incandescence of an eruption column was first reported in 1926, confirming that the crater was well established by that time. A major outburst on 2 November 1927 initiated an interval of virtually continuous eruptive activity, the most violent yet, which lasted until early 1929; ash columns commonly rose more than 4 km, and the nighttime incandescence evoked to valley observers such metaphors as a gigantic torch or a lighthouse atop the Cordillera. The only interruption in this activity is said to have been for a few days before and after the great Talca earthquake of 1 December 1928, the epicenter of which was ~180 km west of the volcano (Lunkenheimer 1932; Bobillier 1932; Fuenzalida 1943). Starting in mid-1929, activity slackened to pre-1927 levels, and for 3 years the intermittent plume emissions were short-lived relative to those of 1927–28 and were separated by longer periods of apparent quiescence.

Although pre-1932 tephra visible on the crater wall today (Fig. 5, Fig. 6) includes bedded black scoria, most of the 1907–1931 activity was phreatic or sometimes merely fumarolic. Photographs taken in 1912 (Vogel 1913) show vapor plumes with only minor ash billowing to heights of 1–2 km above the crater. The only near-vent photograph of activity during the later part of this period (Reck 1933) shows a small 1928 outburst of dark ash, probably phreatic, billowing to a height no more than 300 m above a low rounded cone mantled with coarse ejecta. Quizapu's cone was said to have grown considerably during the activity of 1927–29 (Bruggen 1933; Fuenzalida 1943), but in height this growth cannot have amounted to much, as indicated by

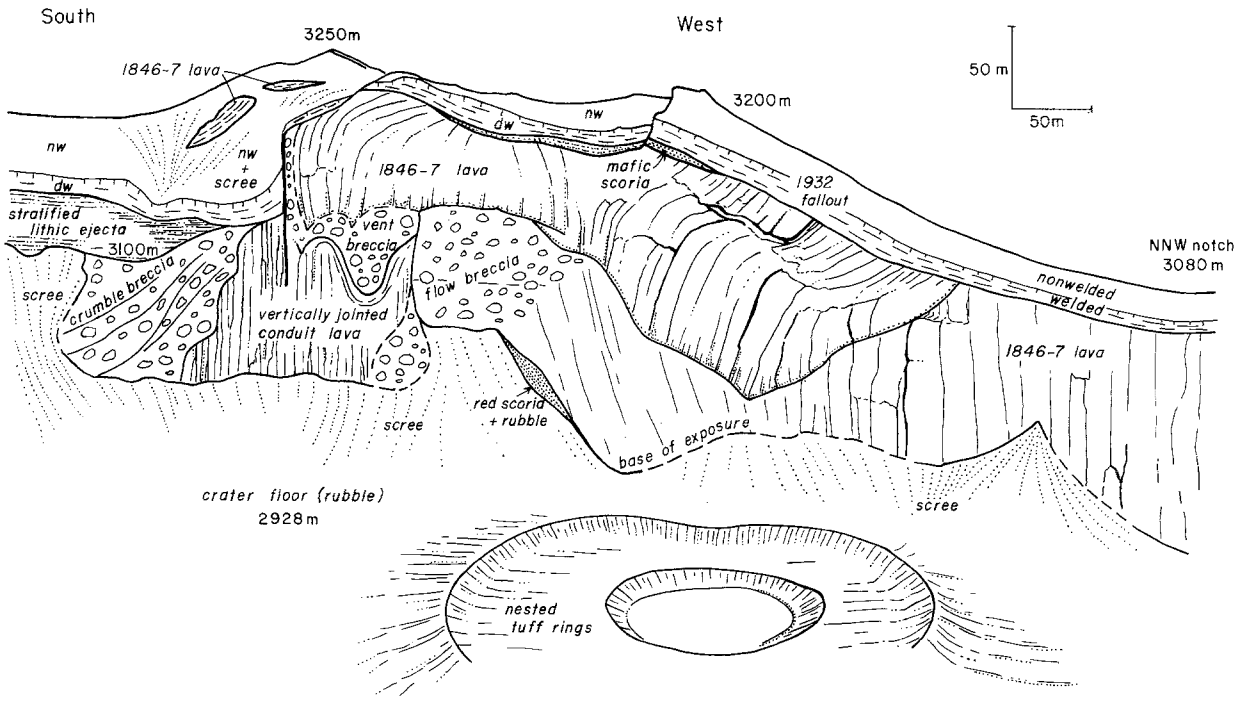

Fig. 5. Sketch of the west interior wall of Quizapu crater. Maximum relief is ~300 m. Part of the effusive vent for the 1846–47 lavas is preserved on the SW wall. A segment of the south rim has been downfaulted. Abbreviations *nw* and *dw* refer to nonwelded and densely welded (commonly eutaxitic) parts of the 1932 fallout on the crater rim

the 1916 photograph cited earlier (Reck 1933), by the limited thickness of pre-1932 ejecta (Fig. 6), and by the fact that 1932 climactic deposits lie virtually on top of 1846–47 lavas around much of the present crater rim (Fig. 3).

Only during later years of this mixed precursory activity was the name Quizapu applied to Cerro Azul's new flank vent. Bruggen (1933) reported that a foreign excursionist sought a local name for the newly active crater from an arriero, who responded in the contracted vernacular of the backcountry: Qui(én) sa(be) pu(es)? (Who knows?). [A variant is: Quizás pues?]

In early 1932, small explosions continued intermittently, but only once or twice was much ash ejected. On 25 January 1932 a black "pine-tree" cloud (Kittl 1933) was reported above Quizapu by observers near Malargüe (105 km E; Fig. 1). Carabineros (police) at Laguna Invernada (Fig. 2) during the first week of April later recalled that the ash clouds had already seemed extraordinary (Bruggen 1950). On the morning of 9 April, an unusual grey-green emission surprised observers, and the volcano began to "bellow like a bull" (Bobillier 1932). The column of "smoke" and vapor grew rapidly that day and was illuminated by a red glow from the crater that night.

Eruption of 1932

A towering white vapor column, probably still tephra-poor, was widely visible against clear skies early in the morning of 10 April, but several contemporary observations suggest that the eruption did not become plinian until well after 1000 h. At about that hour, the first explosions were reported and the white column began to turn dark – according to witnesses in both the Chilean Central Valley and the Argentine countryside north and west of Malargüe (Fig. 1); soon afterward a great umbrella cloud began to form (Bobillier 1932; Kittl 1933; Reck 1933; Fuenzalida 1943). As no arrieros or others are known to have been in the uninhabitated regions anywhere near the volcano at the time, all observations were from afar. Accordingly, the first fallout reported was not in Chile but at the nearest downwind habitations in Argentina, Puesto El Tristan (47 km ENE) and Carrilauquén (62 km ESE), where fine ash began falling about 1300 and coarse "sand" (and sparse pumice lapilli) at 1600 (Kittl 1933). Argentine times are one hour ahead of Chilean.

Viewed from the NE in Argentina, the vertical column promptly spread into a pine-tree cloud, first appearing to be drawn out southward but rapidly expanding eastward, accompanied by "hurricane" winds (Kittl 1933). Viewed from the NW (Curicó and Talca), the column itself consisted of numerous upward-decelerating pulses, and it soon developed a diffuse cloudy halo that slowly spread out (largely northward from this perspective) into an umbrella cloud, above which was maintained a central billowing cloud cap 2–3 km higher (Fuenzalida 1943). Various visual reports of column height ranged from 10 to 30 km; an (unspecified) instrumental measurement from Talca (85 km WNW) gave 16 km at 1130, and a photograph taken at 1600 provided an estimate of 30 km above sea level or ~27 km above the vent (Bobillier 1934).

Fig. 6. East-to-northeast interior wall of Quizapu crater, showing 1846–47 dacite lava overlain by >50 m of dark 1907–31 mafic scoria, both cut by a mafic dike. Rimming the crater is ~20 m of 1932 dacite fallout, the lower half of which is densely agglutinated. This in turn is overlain by ~5 m of light-grey cross-bedded phreatic ash (the undulating light-colored layer at the head of the chute to the right of the dike), capped by several meters of black scoria. Total relief on crater wall below the low east rim is ~150 m. Arcuate tuff ring on the crater floor at the lower left is partly obscured by scree and black ash-covered snow. Beyond the crater rim are a plateau of 1846–47 lava and the lower SE slope of Volcán Descabezado Grande, separated by the head of Quebrada Azul and heavily mantled with 1932 pumice

Explosive detonations were audible from 1000 onward in a number of Argentine settlements but apparently not in Chile until about 1400. For the next 20–24 hours they were heard widely from Concepción to Valparaíso (Fig. 1), but few or none were audible inside an acoustic quiet zone extending out to ~100 km from the volcano (Bruggen 1933, 1950). Within that zone, however, the persistent rattling of windows at Curicó (85 km NNW) was attributed to atmospheric shock waves (Fuenzalida 1943). In Santiago (240 km N), the detonations were at first spaced at 5-second to 1-minute intervals (Vogel 1933; Bruggen 1950) but became virtually continuous after 1700, rattling doors and windows without interruption. The cannonade, which was initially mistaken for distant artillery, attained its greatest intensity in Santiago at 2100–2300, remained prominent until about midday on 11 April, and faded thereafter so that the vibrations were barely perceptible that night. On the Argentine side of the Cordillera, explosions could be heard until as late as 1800 on the 11th (Kittl 1933). Small earthquakes were felt at Curicó (Fuenzalida 1943), and many were recorded instrumentally at Santiago and La Plata, mostly between late evening on 10 April and early afternoon on the 11th (Lunkenheimer 1932; Friedlaender 1933). The sparsity of reports of felt earthquakes may in part reflect the greater prominence of the atmospheric shock effects.

The eruption column and its umbrella cloud were illuminated all night, reportedly in part by incandescence but mostly by spectacular and virtually continuous lightning. Incandescent ballistic ejecta are said to have been witnessed from Curicó (Fuenzalida 1943). In contrast to the effusive eruption of 1846–47, almost none of the accounts mentions the odor of sulfur gases.

Plinian behavior appears to have terminated on the morning of 11 April, but by then the visibility was too poor to be sure. Earthquakes persisted until about 1300, explosions waned after midday, and nothing but *fine* ash is reported to have fallen during daylight hours on the 11th-either at proximal downwind settlements (Carrilauquén) or in the Chilean Central Valley. Our estimate for duration of the plinian phase is thus about 18 hours (1100 to 0500), but it may have been slightly shorter and lesser activity could have lasted as long as 26.5 hours (1030 to 1300).

The ash cloud moved rapidly eastward across Argentina and was initially confined to a sector no wider than ~15°. Fallout began at Carrilauquén (62 km ESE) by 1300 and at Buenos Aires (1125 km E) by 0400 on 11 April. If the average propagation rate (71 km/h) between those locations is assumed for the near-vent region, then the transport time from a position above Quizapu to Carrilauquén would have been slightly less than an hour, implying that the plinian column first penetrated the region of high-altitude wind about noon Argentine time (or 1100 Chilean time).

The rapid initial easterly transport was followed by a much slower expansion and drift of the ash cloud NW across Chile and NE across southern Brazil (Fig. 1); southerly expansion was less extensive. From published accounts, Larsson (1937) constructed an isochron map of the onset of fallout, illustrating both the initially narrow distribution and the gradual expansion. From the perspective of observers in the Chilean Central Valley, the umbrella cloud seemed almost stationary for many hours, but by nightfall on 10 April it had started to expand and descend toward them (Fuenzalida 1943). Fine ash began to fall in Curicó early on the 11th, in Santiago by 1000, and near its apparent NW limit at Quintero (320 km NW) by that afternoon. East of the Andes, fallout did not begin at Mendoza (350 km NE of the vent and ~300 km N of the dispersal axis) until about 1700 on April 11, but by this time the distal downwind ash cloud had already drifted NE over central Uruguay (1400 km ENE; Fig. 1). Although fallout ended on 12 April in Chile, Mendoza, San Rafael, and Buenos Aires (and therefore over virtually all of the initial dispersal area), the continuing NE drift brought fine ash to Rio de Janeiro (2950 km NE) at 1600 on 15 April. The 108-hour difference in arrival times yields a Buenos Aires-to-Rio de Janeiro (1980 km) transport rate of ~18 km/h. The dust cloud reached Cape Town (7300 km due E of Quizapu) on 21 April when a fiery red sunset initiated several months of atmospheric effects all across southern Africa (Jones 1932). The average propagation rate of the tephra front from Quizapu to Cape Town was ~27 km/h, illustrating that even at great distances the due-easterly axial transport remained 50% faster than the oblique off-axis expansion into Brazil (Fig. 1). Dust-enhanced sunsets soon began in Peru, Australia, and New Zealand as well but not in the northern hemisphere (Reck 1933).

The eruption caused great anxiety on both sides of the Andes, but owing to the remoteness of the volcano there were no known deaths or serious injuries and not even much property damage. Much seasonal pasturage in the Cordillera was blanketed with pumice and remains barren, but the few millimeters of ashfall in the Central Valley did not appreciably damage agriculture. Temperature dropped to ~5° C (20°–25° C being daytime normal) during the hours of darkness caused by the ashfall around Curicó on the 11th and in the San Rafael-Malargüe area on the 10th, but the cooling caused little more than consternation. In July 1932 (Fuenzalida 1942) or October 1932 (Bobillier 1934), a pumiceous mudflow from the west cirque of Descabezado Grande led to breakout (and permanent draining) of the Lagunas del Blanquillo (which had been impounded by the 1846–47 lavas; Fig. 2), causing much damage downstream on the Río Maule, apparently the most serious indirect result of the eruption. M. Vogel had warned the authorities as early as 1916 about the hazard of breaching the thin permeable septum of blocky lava impounding the lakes (Riso Patrón 1917; Vogel 1920).

Post-plinian activity

Several overflights and overland expeditions to the eruption site were attempted within 10 days of the plinian event (Bustos 1932; Maass 1932; Bruggen 1933; Reck 1933; Vogel 1933; Fuenzalida 1943), but most were turned back by ash clouds. An aerial oblique photo taken on 12 April shows a cloud of dark ash billowing to ~1 km above the crater and drifting northeastward (Bustos 1932; Reck 1933). Ash emission had largely ceased within 7–10 days, but occasional bursts of ash and detonations were reported as late as 21 April (Bobillier 1932; 1934; Bruggen 1933). It is most likely that the phreatic ash and strombolian scoria layers overlying the plinian deposit on and near the crater rim (Table 1; Fig. 6) were emplaced during this interval.

A team from the University of Chile first reached the crater on 21 April (Bobillier 1932; Bruggen 1933; Fuenzalida 1943). Although interior visibility was limited to the west wall, they reported persistent tremor, tension gashes in the thick (agglutinated) tephra (Fig. 3) on the ventfacing slope of Cerro Azul, and many vigorous fumaroles that generated a crackling sound like a "great pot of chicharrones". By the time of the next reported visit to the rim in February 1934, fumarolic activity had moderated greatly. Small ashclouds were reported (but not investigated) in 1949 and 1967 (Simkin et al. 1981); they were said to have dusted the snowclad cone with fine ash, but we have not with certainty been able to detect any surviving deposits. During our fieldwork in the 1980's, there were no signs of activity other than wispy odorless fumaroles with orifice temperatures in the range 45°–75° C. These remain numerous on the crater floor, walls, and rim, and others were found 750 m NNE of the rim issuing from the 1846–47 lava and ~900 m S of the rim where an extensive area of altered 1932 pumice is exposed at ~3450 m on the north flank of Cerro Azul.

Two weeks after the plinian event of 10–11 April and shortly after cessation of ash emission at Quizapu, activity shifted 6–7 km northward to Descabezado Grande. Two white vapor plumes high on the west flank were first noted sometime in the interval 23–28 April and persisted until at least 1936 (Fuenzalida 1942). This was the first fumarolic activity ever reported at Descabezado Grande in centuries of observation, and it suggests that vertical injection or lateral dike propagation in 1932 took place beneath an extensive area. Reports conflict on the time of initiation, but sometimes between early June and 2 July 1932 (when

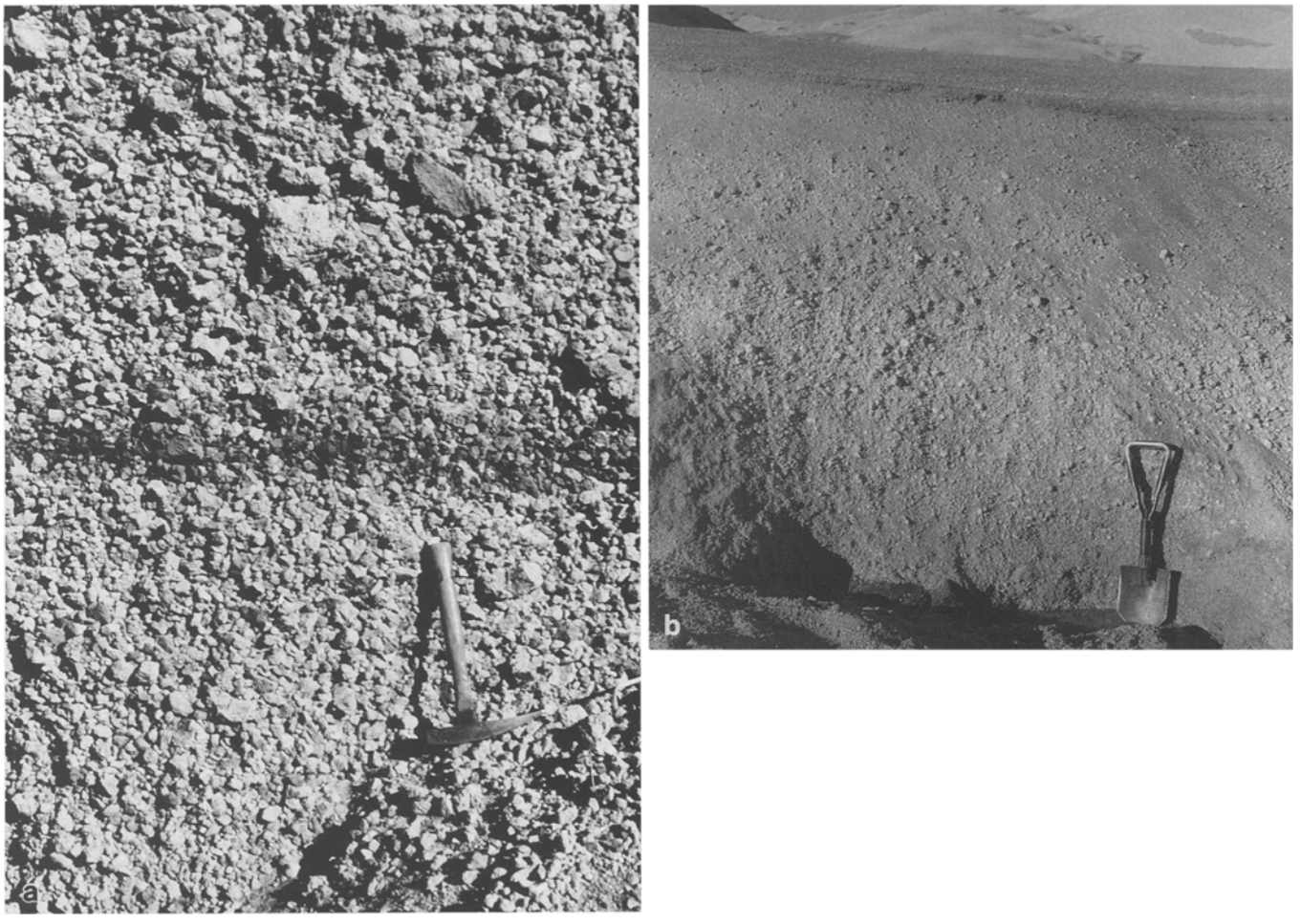

Fig. 7. a Partial section of 1932 fallout in lower Cajón Los Calabozos, 10 km due E of the crater. Deposit is characterized by near-absence of stratification, little change in grain size, sparsity of lithic fragments, and overwhelming dominance of dacite pumice – except in the 8-cm-thick *"brown band"* where andesitic and banded pumice predominate. Such pumice is rare in the plinian deposit above and below this thin layer, which has been traced >30 km eastward to the Argentine frontier. Hammer is ~30 cm long. **b** Natural exposure of a complete 1932 fallout section 10.3 km due N of Quizapu crater; 58-cm shovel rests on till. Plinian deposit is 152 cm thick, weakly graded, coarsest 65–75 cm above the base, poor in lithics and in fine ash, and lacks the "brown band" present only east of the vent. Grainsize data are given in Table 2 (Q-124). Section is capped by a 14-cm layer of darker lithic-rich ash deposited during phreatic eruptions of Descabezado Grande later in 1932

Central Valley towns were dusted with fine ash), a new 600-m-wide crater developed on the upper NNE slope of Descabezado Grande (Reck 1933; Vogel 1933; Bobillier 1934; Fuenzalida 1942). Continuing sporadically well into 1933, dark ash clouds from this crater commonly billowed up to 2 km and rarely to 7–8 km, depositing 5–40 m of stratified, block-rich, poorly sorted lithic ejecta around the rim, ~25 cm of crystal-lithic ash on he summit icecap, and a few tens of cm of finer ash on the lower (principally NE) flanks of the volcano. We have not identified a juvenile component and consider all this activity to have been phreatic. There have been no eruptions since 1933, although acid fumaroles remain active in and near the new crater, and vapor plumes from still higher on Descabezado Grande were reported occasionally during the 1980's (Moreno 1982).

Quizapu Crater

Quizapu is one of the highest known plinian vents, the elevation of its undulating crater rim being 3080–3230 m. The crater floor, at 2928 m, is enclosed by precipitous walls as high as 300 m on the southwest (Fig. 5) but only ~150 m adjacent to its low east rim (Fig. 6). The crater's diameter is 600–700 m at its rim, but only ~300 m at its subcircular floor, suggesting an effective plinian vent radius of ~150 m.

No pre-1846 rocks are exposed inside or adjacent to the crater, which was excavated through the 1846–47 dacite lavas at the site of their own vent. Two dacite lava flows, each as thick as 125 m, are exposed in cross-section on the west wall of the crater where they roll over into a vertically jointed, peripherally brecciated complex (Fig. 5) that appears to be part of their conduit. The upper flow is a remnant of what was probably a small vent dome, and it apparently feeds into the

Table 1. Stratigraphic sequence for Volcán Quizapu

	Unit	Composition	Maximum thickness (m)	Comment
1949(?), 1967				
	Phreatic ash	Nonjuvenile	?	Events uncertain; possible origin of tuff rings on crater floor. Dusting of outer slopes.
1932				
	Terminal scoria fall	Basalt + andesite	6	Largely on E side of crater
	Phreatic ash	Crystal + lithic rich	5	Cross-bedded, lenticular; crater rim
	Post-plinian pyroclastic flow	Dacite	7	Went down Quebrada Azul only
	Plinian pumice fall	Dacite (+ minor rhyodacite)	40	Region-wide fallout; >95% of ejecta
	Intraplinian pyroclastic flows	Dacite	2	Both E and W of crater
	Intraplinian mafic layer	Andesite + banded	0.1	Only E of crater (Fig. 7)
	Initial scoria fall	Andesite + banded	3	Well exposed W of crater; thin to E
1907–1931				
	Scoria falls	Mafic	>50	Only exposed on crater walls
	Phreatic ash and breccia	Lithic-rich	>50	Only exposed on crater walls
1846–47				
	Dacite lavas (Qdl)	Dacite (with mafic blobs)	210	Flows covers 50 km^2
	Precursory ejecta (?)	?	?	May be (poorly) exposed at base of crater wall
Cerro Azul (Holocene)				
	Young silicic lava and ejecta (ra)	Rhyodacite	~25	Largely covered by 1846–47 and 1932 dacites
	Main edifice (az)	Basalt to dacite	—	Stratovolcano with 1100–1500 m relief

Parenthetical symbols *Qdl, ra,* and *az* refer to map units on Fig. 2a

short stubby coulee just west of the cone (Fig. 2). Beneath these flows, near the base of the west wall, is a unique (and poor) exposure of stratified red scoria rich in lithics that could represent the opening phase of the 1846 eruption (Fig. 5). Atop the lava flows, stratified sections of rubbly lithic ash (Fig. 5) and of mafic scoria (Fig. 6), each ~50 m thick, respectively represent the phreatic and strombolian activity during the cone-building interval 1907–1931.

Surrounding the entire crater, the walls are rimmed by 20–40 m of coarse 1932 fallout, predominantly dacitic, that generally grades upwards from cliff-forming eutaxite through tackwelded pumice to loose nonwelded pumice. The deposit, especially its upper 1–2 m, is also sprinkled with denser blocks, both accidental and juvenile, some exceeding 1 m, that exhibit a range of textures from breadcrusted to vitrophyric to devitrified. Granitoids, metamorphics, and pre-1846 lavas make up only a small fraction of the dense ejecta, most of which are either juvenile or were torn from the units exposed on the crater walls.

The 1932 fallout is only half as thick (~20 m) on the east rim, where it fell on the outer slope of the 1907–31 scoria cone, as it is (40 m) on the west-to-southwest rim, where it accumulated atop an 1846–47 lava flow. This proximal asymmetry is contrary to the sense of asymmetry of the main plinian dispersal, which was markedly eastward (Fig. 8). The contrast may have been caused by orifice geometry, by the influence of slope on accumulation, by low-altitude easterly winds, or by the influence of the Cerro Azul edifice on the pattern of winds drawn inward and upward into the eruption column. A similar effect is observed in the dispersal pattern of 1912 ejecta from Novarupta (Alaska), where coarse near-vent material exhibits very strongly asymmetric accumulation to the NE of the vent whereas concurrent dispersal of the main downwind plinian deposit was to the ESE (Hildreth 1987; Fierstein and Hildreth 1992).

High on the west wall of the crater (Fig. 5) a few meters of bedded scoria are sandwiched between the upper 1846–47 lava and 1932 agglutinate. It is not known whether this unique exposure (accessible only by rappeling) represents pre-1932 fallout or the opening phase of the 1932 eruption itself (see Table 1).

Directly atop the main-phase fallout on the crater rim, principally on the east rim and adjacent outer slope of the cone (Figs. 4, 6), lies as much as 5 m of wavy- and cross-laminated crystal-lithic ash that forms several bedding sets emplaced by phreatic surges. These are overlain in turn by up to 6 m of stratified mafic-scoria fall deposits (52–56% SiO_2) that are thick and coarse enough to have survived wind scour within ~1.5 km of the crater. The narrative evidence, though not definitive, suggests that both deposits were emplaced within 7–10 days after the plinian event.

On the crater floor (Figs. 5, 6) are two nested tuff rings, the outer of which has a rim diameter of ~150 m, internal relief of ~15 m, and active fumaroles inside. The inner is 5–8 m deep and is usually filled with snow. Although not visited owing to the hazard of descent, the ring material appears similar to the phreatic surge beds on the rim. As the tuff rings are not overlain by the rim-draping scoria fall, however, they are probably younger, perhaps as young as 1967.

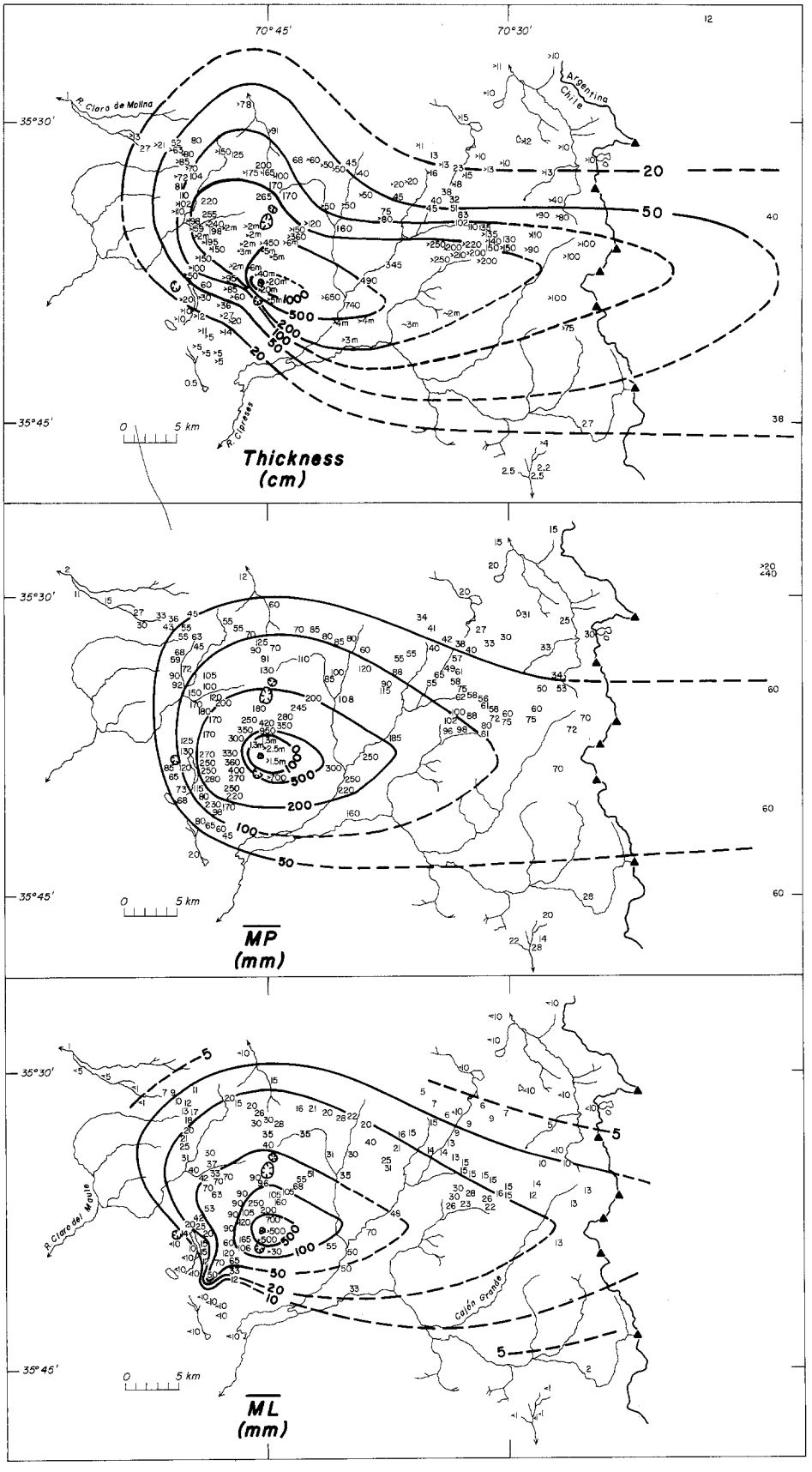

Fig. 8. Proximal isopachs and isopleths of average maximum pumice ($\overline{MP}$) and maximum lithic ($\overline{ML}$) sizes for 1932 fallout. For distal isopachs, see Fig. 1. $\overline{MP}$ and $\overline{ML}$ are averages of 3 axes of 3–5 largest clasts at each station. For locations of craters and drainages in the proximal region, compare the base map with Fig. 2. The area is roadless and uninhabited; data were gathered on backpacking expeditions 1980–91. *Triangles* are peaks along continental drainage divide

The Quizapu cone, externally, has 150–250 m of local relief (Figs. 3, 4). Much of this relief (and most of it on the west side) is contributed by the 1846–47 lavas, which prior to development of the crater in 1907–1910 had evidently stood as a 1-km-wide dome or swell above the conduit (Figs. 4, 5). The phreatic and strombolian cone-building phase (1907–31) raised the edifice only ~50 m, mostly on its east side. Some initial reports suggested that the cone and crater had been enlarged significantly by the 1932 eruption, but enlargement was in fact rather modest. The 1916 and 1928 photos (Reck 1933) show the cone somewhat similar to its present profile, and 1932 deposits elevated the crater rim by only 20–40 m. Syneruptive erosion of the crater walls clearly took place, but lithic fragments in the 1932 ejecta (Table 2) account for only ~40% of the present volume of the crater (which is ~0.04 km^3). No discernible structural subsidence took place either in 1846–47 or in 1932.

An inward-dipping arcuate fault with as much as 30 m displacement has rotationally lowered the SE quadrant of the crater rim, creating the 200-m-wide inner bench and rim promontory visible in Fig. 4. Outboard of this fault, the partially agglutinated fallout, >20 m thick, is cut by a score of cross-slope fractures ranging from mere tension gashes to normal faults having 10-m displacements, all apparently due to downhill extension of the ejecta sheet on the cone's steep SE slope. Similar gashes and downslope pull-aparts, elongate across the slope, are also abundant on the north side of Cerro Azul (Fig. 3), where within ~1 km of its vent the 1932 fallout sheet is also partly agglutinated. These fissures and faults had developed within 10 days after the eruption (Fuenzalida 1943), but they occur only on steep slopes where the fallout was both thick and welded. This suggests that both agglutination and steep topography played roles in developing these shallow structures. In both areas, however, numerous fumaroles, active and fossil, are concentrated along the fractures, suggesting that some of them penetrate deeper than the fallout mantle.

Eruptive products

1846–47 lavas

The dacite lava of 1846–47 consists of ~15 separate blocky flows that cover an area of 50.4 km^2 (Fig. 2). Assigning apparent thicknesses of 25–210 m (mostly 30–125 m) to each of ~50 morphological subdivisions yielded a conservative volume estimate of 4.99 km^3. Although the expanse has not been studied in detail, most flows have been visited and all appear to be similar cpx-bearing hb-hyp-plag dacite having 67–68% SiO_2 (Fig. 12; Tables 4, 5). The flows are widely but variably contaminated by abundant mafic to intermediate magmatic inclusions (e.g., Bacon 1986). These are mostly finely vesicular, ellipsoidal to amoeboid, <1 to 15 cm across, contain olivine and plagioclase phenocrysts, and have crenulate, commonly chilled, margins; most are smaller than 1 cm, but they can make up 1–3% of the lava. The "purest" such inclusion analyzed has 54% SiO_2 (Fig. 12).

Nowhere have we been able to excavate beneath any of the coarsely blocky 1846–47 lavas, so we know little about the extent of accompanying tephra. None has been found atop or adjacent to the lavas, but exposure is poor proximally. Along the south edge of the lava complex 1.6–1.9 km west of the crater, a gully has cut through the thick 1932 plinian deposit (uniquely for the near-vent area), exposing underlying material from Cerro Azul but no ash of 1846–47 age. Near the crater floor at the base of the west wall is an (unvisited) exposure of coarse, lithic-rich, red scoria (Fig. 5), which might either be pre-1846 ejecta from Azul, 1846 lava-flow breccia, or conceivably some vent-opening ejecta of 1846. It appears that the arrieros were correct in reporting that this large volume of dacite erupted with hardly any accompanying fallout.

1907–31 ejecta

The 1907–31 stratified scoria and coarse lithic phreatic deposits, each >50 m thick, are exposed only on the precipitous crater walls (Figs. 5, 6) and have not been sampled. The black bedded scoria, cut by quasi-contemporaneous dikes (Fig. 6) and sandwiched between the 1846–47 and 1932 dacites on the east wall, looks like a section through a small strombolian scoria cone.

1932 ejecta

The great eruption of 1932 started and ended with ejection of olivine-bearing black scoria (Table 1), even though >95% of the 1932 ejecta were hyp-hb-pl dacite (~68% SiO_2; Tables 4, 5). Analyses of initial scoriae are in the range 57–63% SiO_2, whereas terminal scoriae range from 52–60% SiO_2 (Table 4; Fig. 12). The terminal scoria deposit is well exposed on the east rim, where it is as thick as 6 m (Fig. 6).

The initial scoria is apparently exposed on the precipitous west wall of the crater (Fig. 5), and the only other proximal exposure lies 1.6–1.9 km farther west, along a steep gully incised to the base of the thick plinian deposit. As much as 3 m of coarse heterogeneous fallout rich in andesitic scoria bombs and in dacite-andesite banded pumice underlies and grades up continuously into the main dacite plinian deposit. Containing abundant lithics (1846–47 lavas ≫ granitoids) and breadcrusted dacite blocks (both as coarse as 1 m in the lower half), this 3-m mixed interval is largely andesitic near its base and increasingly enriched in banded pumice upward. Fewer than 5% of the clasts are uncontaminated dacite pumice, although a few are present even near the base. As many as half of the juvenile clasts are mixed, as a large fraction of the superficially pure scoria contains streaks and blebs of dacite. The top 1 m has fewer and smaller lithics and tends to be

lightly agglutinated and oxidized. A few cm higher, with neither stratigraphic discontinuity nor noticeable change in grainsize, the deposit becomes lithic-poorer and its juvenile component becomes >95% dacite pumice, remaining so throughout the plinian interval, which is here ~5 m thick.

No other occurrences of the initial scoria fall have been found or excavated in the near-vent region, and at numerous sites 4–10 km NE, N, W, and SW of the vent it is uniformly absent. Along a narrow sector due E of the vent, however, it extends for at least 15 km, and it may be represented 8 km SE of the vent (off-axis) by 4 cm of laminated coarse ash. At 12 km downwind, the basal 15 cm of a 345-cm fallout section still has ~40 wt% scoria and banded pumice and ~11 wt% lithics (mostly 1–4 mm).

The main plinian fall deposit is remarkably uniform (Fig. 7), presumably reflecting an extraordinarily steady eruptive column from the stable pre-existing vent. Away from the cone itself, internal stratification is almost undiscernible and grainsize grading is limited. West of source, the apparent uniformity is supported by sieve data (Table 2) for bottom and top samples that show identical median grainsize ($Md\phi = -1.8$) at 2.5 km SW of the vent and an upward coarsening only from -1.9ϕ to -2.6ϕ at a section 7.4 km NW of the vent. About 10 km north of source (e.g., Fig. 7b; Table 2; Q-124) where thickness is 1.5–2 m, the lowest ~50 cm shows slight inverse grading and the top ~20 cm shows slight normal grading, the coarsest interval occurring at the 30–45% level of the deposit. Eastward (downwind), the early scoria component participates in the inverse grading that characterizes the basal 20–30 cm of sections 3–7 m thick. The coarsest pumice is present by about the one-third point in such sections, but changes are small and only the top ~20% of the deposits tends to show slight normal grading. Approaching the Argentine frontier, where thickness is ~1 m near the dispersal axis, only the bottom ~20 cm and top 10 cm are significantly finer than the rest. North of the axis, 18–35 km from source where the fallout is only 10–40 cm thick, nearly the entire deposit is normally graded - from 1–5 cm lapilli to coarse crystal ash. In a limited area 8–10 km NE of vent, the coarsest tephra is strictly basal (Table 2; Q-135), and the early scoria-rich zone is absent.

At least 95 wt% of the plinian lapilli and blocks are dacite pumice. Lithics make up only 2–3 wt% proximally (even as close to source as 2.5 km), and this declines to <1 wt% within 30 km eastward (on axis) or within ~15 km northwestward. Excluding the initial and terminal scoria falls, the fraction of mafic and banded pumice in the main deposit is nowhere >3 wt%, declines to ~1 wt% by 30 km downwind, and is generally <1 wt% everywhere north and west of the vent. Another juvenile component is frothy rhyodacite pumice (69–70% SiO_2), which constitutes <0.5 wt% of the deposit but is present at all levels and in all sectors. It seems to have erupted persistently and concurrently with the dominant dacite (67–68% SiO_2), showing no preferential concentration near the base of the plinian deposit. Rhyodacite pumice is readily distinguished from the brittler dacite by its greater vesicularity. Density determinations give 0.26–0.30 g/cm^3 compared to 0.53–0.78 for the coeruptive dacite pumice. The rhyodacite also has a tendency to form pumice lapilli of high aspect ratio (commonly 4:1 but as large as 9:1) that can sail to great distances from vent. This phenomenon could severely bias maximum-pumice data, especially if only the longest instead of all three axes of each clast were measured.

A remarkable departure from the plinian compositional relations just outlined is the "brown band" (Fig. 7a), a thin downwind layer of banded and andesitic pumice, that occurs without any grainsize change within the coarsest interval of the plinian deposit. It is not present north or west of the crater, but is has been traced eastward from Quebrada Azul to the Argentine border. Within ~12 km of source, the layer is 7–10 cm thick and occurs at the 25–33% level of 3–7 m sections. On axis, 20–25 km east of the vent, where the deposit is 1.5–2.5 m thick, the brown band is 4–6 cm thick and occurs at the 37–44% level. At similar distances but north of the dispersal axis, the layer occurs at the 45–50% level and gradually thins to a single lapillus, but it remains well defined until deposit thickness is <40 cm. Although making up only 2–3% of the fallout thickness, its changing position provides a basis for a more detailed analysis of the fallout pattern than undertaken here.

Contacts of the brown band are abrupt (irregular only at the scale of individual lapilli). It contains very few dacite pumice lapilli, and the enclosing plinian dacite contains only 1–3 wt% of banded and andesitic pumice like that comprising the band. A macroscopically homogeneous pumice clast (Q-1; Table 4) from the band gave 57.4% SiO_2. The band evidently resulted from transiently enhanced access of andesitic magma to the conduit during the interval of peak discharge, promoting extensive mingling with the coerupting dacite but without itself significantly affecting the discharge rate. The andesitic magma was similar to part of the material that fed the pre- and post-plinian scoria falls, but it bled only sparingly into conduit flow during evacuation of most of the plinian dacite.

1932 lithics

Componentry yields 2–3 wt% lithics at 2.5–5 km from vent, 1–2 wt% at 5–28 km, and ~0.1 wt% at 100 km downwind (Table 2). Samples from greater distances have fewer still, but at <250 μm (2ϕ) true lithics become difficult to distinguish from fragments of juvenile scoria and breadcrusted dacite, both of which are present in similarly small concentrations. Lithics may exceed 5 wt% of the fallout within 1–2 km of the crater, but no attempt has been made to quantify components accurately in this coarse material. As far as 15–20 km downwind, the lower one-third of the plinian deposit is generally richer in lithics than above, but there is no systematic difference north or west of the vent. The

Table 2. Representative physical data for 1932 pyroclastic deposits

No.	From vent		Mdϕ	σϕ	Wt % <1 mm	Wt % < 63 μm	Bulk[a] Density	Wt % Lithics	Wt % Crystals	Notes
	km	Azimuth								
Plinian fallout										
Q-49A	2.5	244	−1.85	1.03	12.3	2.2	0.59	2.3	6.2	Lower half
Q-49B	2.5	244	−1.82	1.10	15.5	2.1	0.60	3.2	7.0	Upper half
Q-48	4.35	225	−1.35	2.07	29.5	7.5	0.63	3.4	11.3	
Q-43	5.25	212	−0.69	2.77	41.0	11.5	0.68	1.4	11.9	
Q-77A	7.4	323	−1.91	1.81	13.4	0.8	0.57	1.9	5.7	Lower half
Q-77B	7.4	323	−2.59	1.50	5.9	0.7	0.56	1.5	2.7	Upper half
Q-23	7.7	310	−2.82	1.61	8.3	0.35	0.55	1.8	4.3	
Q-135A	8.8	52	−4.08	1.05	6.1	1.3	0.49	0.7	3.5	Basal 15 cm; coarsest
Q-135B	8.8	52	−1.50	1.67	20.1	0.03	0.65	0.8	13.3	Interval 30–40 cm above base
Q-124A	10.3	0	−1.50	1.79	22.2	0.71	0.52	0.8	14.4	Basal 5 cm
Q-124B	10.3	0	−1.50	1.85	21.6	0.03	0.59	0.6	14.6	Basal10 cm
Q-124C	10.3	0	−2.11	2.22	23.1	0.13	0.65	1.5	13.9	Interval 65–75 cm above base; coarsest
Q-124D	10.3	0	−1.07	1.43	25.9	0.70	0.71	4.0	14.7	Top 10 cm
Q-24	15.7	322	−0.41	1.41	41.8	0.05	0.72	0.8	21.0	
Q-12	17.5	66	−3.63	0.89	3.9	0.43	0.50	1.7	2.2	Top missing
Q-15	21.0	60	0.23	2.24	53.9	0.59	0.71	1.2	28.2	
Q-13	27.5	90	−1.65	1.06	11.8	0.04	0.49	1.1	10.2	Top missing
Q-101	71	45			99.9	65.5	1.10	0.1	13.1	
Q-104	105	35			100	55.9	1.02	—	7.8	
Q-102A	106	86	1.61	0.84	99.9	7.4	0.91	<0.1	47.1	Lower third
Q-102B	106	86	1.25	0.77	99.9	6.2	0.73	<0.1	27.1	Middle third
Q-102C	106	86	1.49	0.74	99.9	3.5	0.82	<0.2	46.4	Upper third
Q-103	112	90	1.50	0.57	99.6	2.6	0.97	tr	59.2	
Q-100	123	61			99.7	69.2	1.05	—	17.1	El Sosneado
Q-107	560	89			100	64.5	1.05	tr	6.5	Caleufú
Q-106	570	87			100	55.9	0.92	tr	6.9	Ingeniero Luiggi
Q-108	635	90			100	62.8	1.04	tr	7.8	General Pico
LO	810	62	6.4	0.9	100	100	>0.95	tr	5	La Olguita (Larsson 1937)
BA	1125	87	6.5	1.5	100	88.6	>0.87	tr	7	Buenos Aires (Kreutz and Jurek 1932)
Pyroclastic flow										
Q-86	1.3	150	0.79	2.91	57.8	12.1	1.35	20.8	37.3	At end of plinian phase
Crater-rim surge										
Q-90	0.1	90	3.06	0.97	99.9	22.4	1.43	56.0	16.3	Typical 5-cm layer; post-plinian

[a] Bulk density was determined in the laboratory after drying by tapping-compaction of tephra in a 1000-cm³ graduated cylinder. Some distal ash was coherent enough to be carved in the field into cubes or other pieces of readily measurable volume; dry weight was later measured in the laboratory

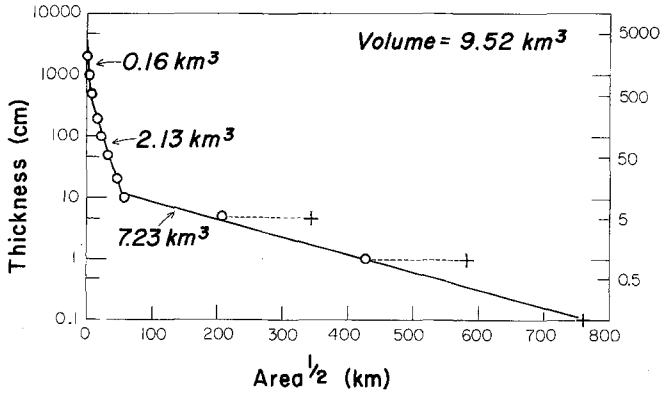

Fig. 9. Plot of thickness (log scale) vs square root of isopach area (Figs, 1, 8) for 1932 fallout, after Pyle (1989). Volume (9.5 km³) is calculated by integration under three line segments as shown; the two *inflection points* are thought to represent (1) the outer limit of significant ballistic influence (thickness between 10 m and 5 m) and (2) the range where fine plinian ash begins to undergo different settling behaviour (thickness ~10 cm), probably involving particle aggregation. *Crosses* (+) represent areas of uncompacted fallout given by isopachs of Larsson (1937); *circles* are based on our 1980–1991 data for compacted tephra

"brown band" does not differ from the enclosing dacite fallout in its (sparse) lithic content.

Well over 90% of the accidental lithics are devitrified or glassy 1846–47 hb-dacite lava, mostly torn from the crater walls. Small amounts of oxidized scoria and hydrothermally altered lava probably also came from the walls - and perhaps some of the latter from the deeper conduit. Fragments of mafic lava from Cerro Azul or older units are sparse, and Mesozoic metamorphic rocks are very rare in the 1932 ejecta. Fragments of granite, granodiorite, and diorite from the underlying Invernada pluton (Fig. 2) are only rarely partially melted, tend to be larger than other lithics, and make up ~1% of the lithics proximally and a smaller fraction distally owing to granular disaggregation.

On the basis of componentry (Fig. 11), bulk densities (Table 2), and fallout volumes calculated for each isopach (Fig. 9), we estimate a total of 0.017 km³ of accidental lithic ejecta, which amounts to only 0.4% of the fallout (4.05 km³ DRE) and 38–43% of the crater volume (0.039–0.044 km³). The uncertainty in total lithic

fraction is thought to be only 10–20%, because a large proportion of the tephra is distal (Fig. 9) where lithics are very sparse (0.01–0.1 wt%). The fact that the crater had been reamed through massive lavas prior to the 1932 eruption permitted an efficient circular plinian vent to evolve quickly with little additional excavation or spalling, thus leading to one of the lithic-poorest plinian deposits on record. By contrast, the comparably voluminous plinian Layer A at Novarupta (Alaska), which represents the opening phase of an eruption that reamed a new vent through nonvolcanic basement rocks, contains a mass fraction of lithics 20 times greater than that at Quizapu (Fierstein and Hildreth 1992).

Near-vent ejecta and pyroclastic flows

No evidence has been found for any initial surge, fine ash, or vent-opening blast. The crater was already established and the eruption began with a coarse andesitic scoria fall that evolved continuously into plinian dacite. Within ~1 km of the rim, the very coarse dacite fallout is vaguely stratified (especially east of the crater), probably owing to discharge velocity fluctuations that affected near-vent ballistic ejecta and column-margin fallback material but not the regional fallout from higher parts of the convective column and the umbrella cloud. Dense blocks, both accidental and breadcrusted, are sprinkled throughout the synplinian rim deposit and are most abundant at and near its top, presumably reflecting faltering of the column at the close of the plinian phase; blocks as large as 2–3 m are common just beyond the NE toe of the cone. The degree of agglutination of the dacite fallout on and near the rim fluctuates vertically but is generally densest in the lower half of the 20–40 m deposit, creating an abrupt ledge that almost encircles the crater. Near-vent ejecta remobilized from steep slopes outside the crater at times of heavy rainfall or snowmelt occasionally (still) produce slurries that deposit sinuous leveed tongues of coarse pumice, some as long as 6 km.

Intraplinian pyroclastic-flow deposits 0.3–2 m thick are exposed in gullies both W and SE of the crater but only out to ~2 km from source. Although rich in dacite pumice (and derivative crystals), these small ignimbrites contrast with the synchronous plinian deposit in being rich in lithic fragments as well (e.g., Q-86 has 21 wt% lithics; Table 2). Perhaps they reflect wall-spalling events that led to local collapse from barely above the rim of lithic-loaded parts of the column periphery, without having any significant effect on steady discharge of the interior of the column.

A larger pyroclastic flow, also rich in lithics and in coarse dacite pumice, went down steep Quebrada Azul at the very end of the plinian phase. As thick as 7 m down at the Rio Barroso (Fig. 2) 7–8 km E of the vent, this ~0.01-km^3 ignimbrite exhibits degassing pipes and fumarolic alteration, and it rests on the normally graded upper part of the plinian deposit, which is missing only its topmost few cm. Just beyond the ignimbrite margins, the plinian fallout grades up to an additional ~5 cm of white 2-mm pumice granules and is overlain by (and slightly mixed with) as much as 4 cm of tan vitric coignimbrite ash. These relations suggest that ash-flow emplacement was essentially synchronous with termination of plinian activity.

On the east rim (Fig. 6) is a well-sorted, pale-gray deposit ($\sigma\,\phi \sim 1$) of cross-laminated crystal-lithic ash, altogether up to 5 m thick, consisting of numerous truncating bedsets and enclosing a few lenses of remobilized pumice and lithic lapilli. Componentry for a typical layer (Q-90; Table 2) gave 56 wt% lithics and 16 wt% crystals, median grainsize being only ~0.12 mm. As olivine is common and tiny mafic scoriae make up 10–15 wt% of the ash, the deposit may well contain a phreatomagmatic contribution, but most of the material appears to be vent-filling debris that was rejected as weak surges when groundwater access to the conduit and crater floor promoted steam explosions during the days immediately after 10–11 April. The dark cloud of ash billowing to ~1 km above the crater photographed from the air on 12 April (Reck 1933) and the ash clouds that turned back the first three parties that attempted to reach the crater overland (prior to 21 April) probably represent this phase of activity.

The crystal-lithic ash is draped by a black scoria-fall deposit thought to be the final emplacement unit at Quizapu in 1932 – excluding perhaps one or both of the crater-floor tuff rings (Fig. 5) of unknown age. The stratified scoria is as thick as 6 m on the SE rim, is essentially confined to the east half of the cone, and has been found only as far as 1.5 km (SE) from the rim. The remnants there are only ~50 cm thick and farther away have been removed by erosion. On and adjacent to the cone, the deposit is nonagglutinated, contains small fractions of breadcrusted and re-ejected welded dacite blocks, and is rich in coarse mafic bombs, many shattered, some fusiform, and a few that splattered on impact. True lithics are fewer than 10% but bomb-rind fragments make the fraction seem much larger. Compositions of homogeneous-appearing bombs so far analyzed range from 52 to 60% SiO_2.

Dispersal of 1932 fallout

Thickness

Thickness variation of the plinian deposit is shown in Figure 1 and in Figure 8, which also gives isopleths of average maximum-pumice ($\overline{MP}$) and maximum-lithic ($\overline{ML}$) clast distribution. Because most of the volume fell in populated areas on land, the 1932 fallout could be one of the most complete plinian deposits known. Unfortunately, however, efforts to record thicknesses in 1932 were unsystematic in Argentina and virtually nonexistent within 45 km of the vent. We have now measured ~180 sections in Chile (Fig. 8), and our 30-location reconnaissance efforts on the Argentine pampas have better defined the distal isopachs. Kittl (1933) published his own thickness measurements for western

Argentina 45–250 km from vent and added to these his compilation of railroad-company reports for ~180 stations in central and eastern parts of the dispersal sector, 250–1125 km from vent. The latter data were reported by numerous individuals, represent estimates for uncompacted (or variably compacted) tephra, and in many cases show poor consistency among nearby locations. Larsson (1937) did no fieldwork himself but constructed an isopach map based principally on Kittl's compilation and partly on a variety of other published sources. Figure 1 shows Larsson's isopachs for uncompacted fallout as well as our tentatively revised isopachs for the compacted ash. Compaction has approximately halved Kittl's thicknesses in distal areas, but within the 10-cm isopach (where crystals and pumice granules are abundant) compaction has been insignificant.

Kittl (1933) noted that the deposit was unstratified but that, where 10–15 cm thick, the bottom 0.5 cm and top ~1 cm were somewhat finer grained, in accord with our own observations as far east as Malargüe (Fig. 1). More distally, however, neither he nor we noted any grading of the fine-grained deposit. Kittl also pointed out the progressive downwind decrease in the proportion of pumice fragments and in crystal/glass ratio that Larsson (1937) later termed "aeolian differentiation."

Kittl additionally documented the (probable) existence of a secondary thickness maximum 550–700 km from vent (Fig. 1) and mentioned the observed clustering of freshly fallen fine-ash particles, although he did not link these phenomena. Larsson (1937) tried to rationalize the secondary thickness maximum by appealing to atmospheric turbulence induced by the Sierra de Córdoba >250 km farther north, but (if real) the downwind thickening is more likely to have been caused by premature fallout of fine ash as larger aggregates, locally concentrated by atmospheric moisture or electrostatic attraction. Such a secondary thickness maximum was recorded ~325 km downwind by Sarna-Wojcicki et al. (1981) for the 18 May 1980 ashfall from Mount St. Helens, and it has generally been attributed to such particle aggregation (Sorem 1982; Carey and Sigurdsson 1982; Brazier et al. 1983). Aggregation of fallout particles at La Plata (1160 km E of Quizapu) was indeed described by both Dartayet (1932) and Lunkenheimer (1932), who measured clusters (copos) as large as 1 mm even though >98 wt% of the ash particles were smaller than 0.1 mm (Kreutz and Jurek 1932). Dartayet pointed out that these loosely structured aggregates imparted an apparent thickness to the newly fallen deposit that was 5× greater than after disaggregation and compaction in the laboratory (0.14–0.17 mm at La Plata). No contemporary examination of newly fallen ash in the area of secondary thickening was reported and (as these fragile clusters readily disaggregate; Sorem 1982) we find no direct evidence for them there today. Nevertheless, 56–65 wt% of the fallout sampled in that area (Table 2; Q-106 to 108) is finer than 63 μm (4ϕ), and the grainsize distribution is similar to that in the 1980 secondary maximum east of Mount St. Helens (Carey and Sigurdsson 1982). It is hoped that ongoing work will clarify both the reality and mechanism of the downwind thickening. Some doubt persists concerning the reality owing to erratic local variation of the thickness data compiled by Kittl (1933), the subsequent compaction and erosion, and the sparsity of both 1932 data and surviving ash deposits along the narrow axial region of the fallout sector across the arid windscoured pampas between Malargüe and General Pico (Fig. 1).

Proximal isopachs (Fig. 8) define both the principal easterly dispersal sector and a subsidiary lobe to the NNW. To the east, the 5-m isopach extends ~12 km, the 1-m isopach ~40 km, and the 10-cm isopach >130 km downwind. Thinning of the deposit is most abrupt SW of the crater, from 40 m to <1 cm within 10 km, presumably reflecting a strong component of wind from that direction at all elevations throughout the eruption. Westerly expansion of the ash cloud was limited, as only 8 mm (uncompacted) accumulated at Curicó and none at Talca (both 85 km from source; Fig. 1). The fine ash that fell on populated areas to the NW (all beyond the 1-cm isopach; Fig. 1) only began falling during the morning of 11 April, at least 18 hours after onset of the plinian phase. Relaxation of a northwesterly component of the wind seems required at some elevation in order to account for this delayed expansion of the umbrella cloud to the NNW. It is not certain whether the NNW lobe evident in isopachs for the thick proximal pumice fall (Fig. 8) also in part reflects a second-day wind shift.

Preserved as a continuous sheet that thickens exponentially to 20–40 m at the crater rim, the 1932 ejecta provide one of the world's best exposed examples of a proximal plinian deposit. Most plinian deposits (Walker 1981a) are much more complex proximally owing to intercalation of pyroclastic flows and surges; moreover, because of erosion, burial, or caldera subsidence, the kind of proximal record preserved at Quizapu is usually lacking. We emphasize that the Quizapu cone is largely a pre-1932 constructional feature, not a 1932 pumice cone. The slight additional thickening owed to a ballistic contribution within ~3 km of the vent causes only a minor inflection in the exponential plinian thickening curve (Fig. 9).

Volumes

Areas within the isopachs of Figures 1 and 8 were plotted following Pyle (1989). Using the method of Fierstein and Nathenson (1991), deposit volumes were then obtained by integration under three, apparently discrete, line segments (Fig. 9), the distal segment integrated to infinity. The 9.52 km^3 tephra volume is thought to be conservative and is only half that obtained by using the 5-cm and 1-cm isopachs of Larsson (1937) for the newly fallen, uncompacted ash (Fig. 9).

Inflections between the segments in Fig. 9 are interpreted here to reflect (1) the outer limit of a significant ballistic contribution, only a few km from vent, and (2) the transition from coarser fallout rich in pumice clasts

and crystals to finer fallout dominated by glass shards. Because the vitric fraction finer than ~0.25 mm is strongly affected by atmospheric turbulence and thus held aloft longer, it can be wind-dispersed to greater distances. More important than size alone, however, the discontinuity in particle *shape*, from quasi-equant pumice clasts and crystals to highly irregular vitric shards, probably controls the discontinuity in fall behavior and settling times that results in the exponential thinning curves of contrasting slope (Fig. 9). The predominantly vitric ash beyond the 10-cm isopach was also subject to clustering (particle aggregation), which would promote premature fallout and overthickening that may have enlarged somewhat the areas included within the 5-cm, 1-cm, and 0.1 cm isopachs. Such an affect, however, is likely to have provided only a second-order contribution in causing the drastic medial-distal inflection of Figure 9.

Similar inflections, remote from source and clearly beyond the range of ballistic effects, have sometimes been attributed to contributions of co-ignimbrite ash to the distal fallout. At Quizapu, however, virtually all of the fallout is unequivocally of plinian origin, as the associated pyroclastic flows are only trivial in volume (~0.01 km^3). Fine-grained plinian ash, decoupled from the coarser fallout and subject both to clustering and to being maintained aloft by atmospheric turbulence, has been called "co-plinian ash" by Fierstein and Hildreth (1992), by analogy with comparably decoupled "coignimbrite ash".

Bulk density determinations for samples of 1932 fallout are given in Table 2. The values are in the range 0.5–0.7 g/cm^3 within ~30 km of vent and tend to rise with distance. Beyond the limit of pumice granules (just beyond the 10-cm isopach downwind), values for the naturally compacted ash generally exceed 1.0 g/cm^3. As ~75 vol.% of the ejecta lie outside the 10-cm isopach (Fig. 9), relatively high bulk densities (0.9–1.1 g/cm^3; Table 2) thus characterize most of the deposit. Because we are primarily interested in the magma volume equivalent to 9.52 km^3 of ejecta, we used a density of 2.4 g/cm^3 appropriate to dacite magma for calculating (per isopach) a pre-vesiculation volume of 4.05 km^3. Of this total, ~0.017 km^3 consists of accidental lithic fragments, leaving ~4.03 km^3 of magma erupted on 10–11 April 1932 (Table 3).

By comparison, the volume of the 1846–47 lavas is conservatively estimated (as described above) to be 4.99 km^3. The poorly exposed lithic-rich ejecta and scoria that accumulated at Quizapu between 1907 and 1931 amounted to no more than 0.1 km^3, probably much less.

Clast size distribution

Pumice and lithic blocks >1 m are scattered within ~1 km of the crater rim on all azimuths but preferentially in the NE quadrant. The isopleth maps (Fig. 8) show that pumice blocks >10 cm fell as far as 22 km downwind but only as far as 10 km in the NNW lobe and <7 km to the SW. Corresponding distances are ~80 km, 23 km, and 12 km for 1-cm pumice and ~40 km, 14 km, and 7 km for 1-cm lithics. The southwesterly salient in the $\overline{ML}$ isopleths (Fig. 8) does not show up in the thickness or $\overline{MP}$ data. Although it is defined by only 8 localities, it appears to be real and probably represents some kind of spalling event on the crater wall that produced a directed shower of ballistic lithic fragments.

The isopleth maps in Fig. 8 are based on a clast-size measurement that is somewhat more conservative than in many such studies. Instead of measuring only the maximum length of each clast, we average the lengths of the 3 principal axes of each. This method reduces the importance of disc-shaped clasts that sail to anomalously great distances, notably shale fragments and, at Quizapu, some of the rhyodacitic pumice clasts. For example, where the average maximum-pumice clast is ~10 cm, one can sometimes find a few as large as ~18 × 14 × 4 cm. Assigning such a clast its a averaged dimension of 12 cm distorts the grand average (for the 5 largest clasts) much less than would counting it as 18 cm. An even better measure of comparable *masses* might be $(18 \times 14 \times 4)^{1/3} = 10$ cm. Our methods yield $\overline{MP}$ and $\overline{ML}$ values that are 10–20% smaller than those based on maximum dimensions alone.

Areas enclosed by the isopleths and isopachs of Figure 8 are compared with corresponding data for several other plinian deposits in Fig. 10. Each panel provides an independent measure of dispersive power, but the rank order of the various deposits is not identical by the three different criteria. Moreover, the striking inflection

Table 3. Volcanological data for 1932 plinian eruption[a]

Vent radius	130–170 m
Volume of ejecta	9.52 km^3
Volume DRE	4.05 km^3
Volume of lithics	0.017 km^3
Volume of magma	4.03 km^3
Duration	18–25 h
Peak MER (SCS)	$0.9–2 \times 10^8$ kg/s
Peak MER (WW)	$1.2–2.5 \times 10^8$ kg/s
MER (18-h avg) magma	1.5×10^8 kg/s
VER (18-h avg) magma	6.2×10^4 m^3/s
Column height (SCS)	28–32 km
Column height (WW)	25–28 km
Column height (visual)	27–30 km
Weight % ejecta <1 mm	82%
Weight % ejecta <63 μm	47–56%
Volume % beyond 1-cm isopach	17%
Peak wind velocity (SCS)	30–35 m/s
Observed transport velocity to Buenos Aires	20 m/s

[a] SCS refers to the methods of Sparks (1986) and Carey and Sparks (1986) for a temperate atmosphere, using data from the lithic and pumice isopleths of Fig. 8 and a magma temperature of 850° C (Fig. 15)
WW refers to the methods of Wilson and Walker (1987), assuming 3–5 wt% magmatic water and the vent radius given above
MER is mass eruption rate of magma; VER is volumetric eruption rate, in terms of dense-rock equivalent (DRE) of magma having a density of 2.4 gcm^{-3}

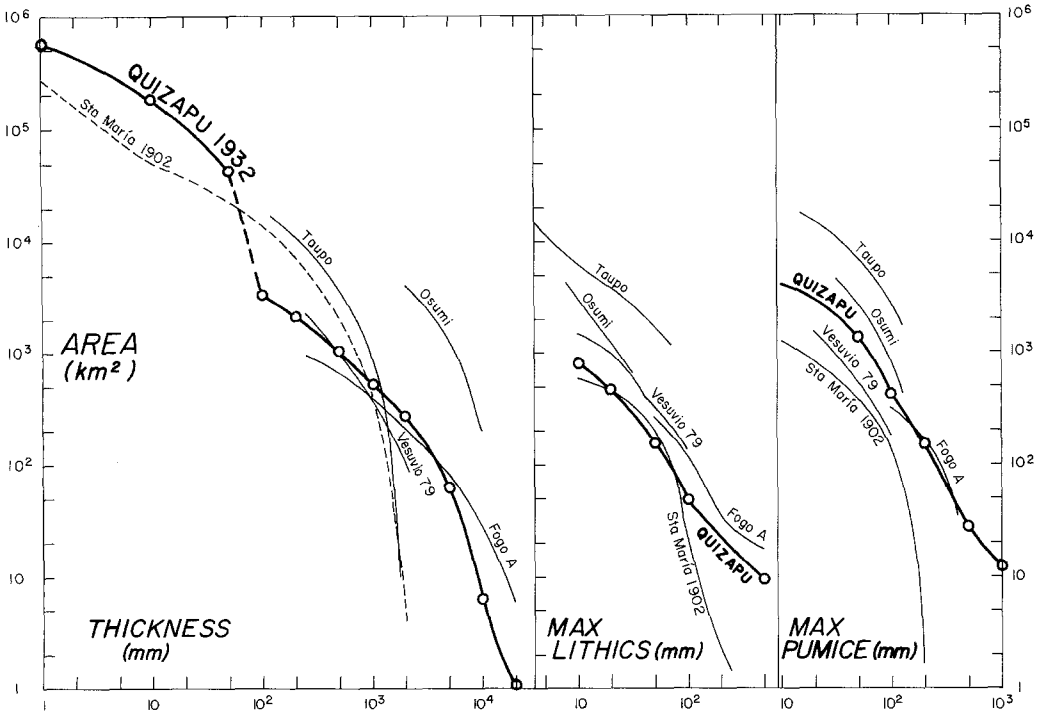

Fig. 10. Areas in km^2 enclosed by thickness isopachs and isopleths of maximum pumice ($\overline{MP}$) and maximum lithic ($\overline{ML}$) sizes, all in millimeters. For comparison, data are shown for five other well-characterized plinian eruptions: Osumi (Kobayashi et al. 1983); Fogo-A (Walker and Croasdale 1971); Taupo (Walker 1980, 1981a); Vesuvio 79 (Lirer et al. 1973; Sigurdsson et al. 1985; Carey and Sigurdsson 1987); and Santa María 1902 (Williams and Self 1983)

between the 10-cm and 5-cm isopachs in both Figures 9 and 10 suggests a need for distinguishing between the dispersal characteristics of proximal-to-medial pumice falls and those of downwind fine ash, whenever data are obtainable for the latter.

Dispersal and fragmentation indices revised

Use of Walker's (1973, 1981a) indices of dispersal (D) and fragmentation (F) should be discouraged, because they are necessarily based upon arbitrary choices for a deposit's maximum thickness (T_{max}), which is often lost and commonly hard to define. At Quizapu, where exposure and preservation are excellent, should T_{max} be taken as 40 m (on the upwind rim), as 20 m (on the downwind rim), or as 10 m (beyond significant ballistic effects)? For these choices, D (= Area enclosed by the 0.01 T_{max} isopach) would be 1200, 2100, or 3300 km^2, respectively, an unacceptably wide range for useful comparisons of eruptive dispersal. A similar objection afflicts determination of F (= wt% finer than 1 mm where the 0.1 T_{max} isopach crosses the dispersal axis). The point here is not to criticize Walker's pioneering innovations but to point out that, since introduction of the methods of Pyle (1989) and of Fierstein and Nathenson (1991), better criteria for comparing dispersal and fragmentation have become readily available.

For example, for proximal-to-medial fallout, a useful dispersal index might be the ratio of areas enclosed by the 20-cm and 1-m isopachs; values are ~4 for Quizapu, ~7.5 for Vesuvius 79 A.D., and ~11.5 for the Taupo plinian. These isopach choices are arbitrary, but reliable data are usually available for this thickness range, and Walker's goal of providing a normalized index largely independent of volume is retained while the problems of distal inflections and of defining T_{max} are both avoided. For comparing the dispersal of finer ash, the wt% of the whole deposit beyond the 10-cm (or 1-cm) isopach provides a useful index; for Quizapu, these values are 75% and 17%, respectively. Similarly, a widely applicable index of fragmentation would simply be the wt% of the whole deposit finer than 1 mm (or 63 μm); for Quizapu, these values are 82% and 47–56%, respectively (Table 3).

Componentry and sorting

Grainsize data, bulk density, and the proportions of lithics and free crystals are given in Table 2 for 31 samples of the 1932 deposits. Histograms illustrating the grainsize distribution and componentry for a selection of these are presented in Fig. 11. Along the dispersal axis downwind, median grainsize is ~15 mm at 20 km, 3 mm at 30 km, 0.35 mm at 100 km, and ~0.01 mm at 1000 km. Sorting ($\sigma\phi$) tends to improve with distance, as expected, but it is also very good in some proximal pumice sections that are poor in crystals and lithics (Table 2).

Lithic content of the fallout exceeds 2 wt% only within 5 km of vent. It falls to <1 wt% within 15 km NW or within 30 km eastward (along the dispersal axis). By 100 km downwind, the lithic content is negligible (<0.1 wt%), although sub-63-μm lithics were transported in trace amounts even as far as the Atlantic coast.

The dominant dacite pumice erupted in 1932 contains ~16 wt% phenocrysts (Table 5). The free crystal content of the fallout exceeds this only within what ap-

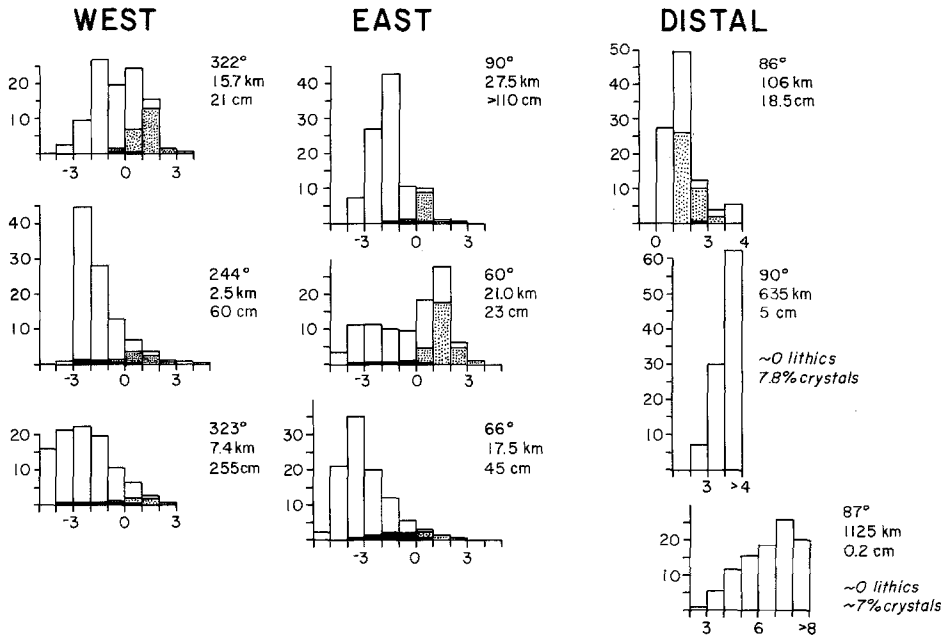

Fig. 11. Histograms illustrating grainsize spectrum and componentry (wt %) for selected samples (Table 2) west, east, and remote from Quizapu. Azimuth and distance from the crater and deposit thickness are shown for each sample. Lithics shown *black*, free crystals *stippled*, and pumice-plus-vitric-shards *white*. Deposit is unusually poor in lithics. Grainsize is shown at one-phi ϕ intervals, where $\phi = -\log_2$ (grainsize in mm); each size class is denoted by the mesh size that retains it

pears to be an annular zone 12–20 km from vent to the north and west; eastward along the dispersal axis, however, the crystal-enriched zone stretches out from ~20 km to at least 125 km downwind. Inboard of this zone, most crystals are retained in pumice clasts, whereas outboard the proportion of vitric shards progressively increases at the expense of free crystals. Nonetheless, even at great distances (560–1125 km) downwind, the ash has 5–8 wt% crystals, most of them finer than 63 μm (Table 2).

From the data of Table 2 and Fig. 9, we estimate that 82 wt% of the whole Quizapu plinian deposit is finer than 1 mm. This compares with 85, 81, and 76 wt% finer than 1 mm for three Holocene rhyolitic plinian deposits in New Zealand studied in detail by Walker (1980, 1981b). Because most of the Quizapu deposit fell on land, we can further estimate with some confidence that between 47 wt% and 56 wt% of the fallout is finer than 63 μm (4ϕ). It is unlikely that phreatomagmatic effects contributed significantly to fines production since (1) the proximal deposits are poor in fines, and accompanying pyroclastic flows and surges are volumetrically trivial, (2) nearly all the dacite pumice is well vesiculated, and (3) the crater has contained no lake, neither then (Vogel 1913, 1920; Fuenzalida 1943) nor now, being situated on a high saddle having little catchment for groundwater recharge. The seemingly high fraction of fine ash may actually be common for plinian deposits, the downwind records of which are rapidly eroded or lost at sea.

Column Dynamics

Vent radius, exit velocity, and magmatic volatile content together control the mass eruption rate, which is the principal determinant of column height (Wilson et al. 1980; Wilson and Walker 1987). Column height in turn, along with wind patterns, strongly influences column geometry, expansion, and clast dispersal (Sparks 1986; Carey and Sparks 1986). The Quizapu crater is nearly circular, optimum for minimizing frictional drag and for application of the theoretical column models. Crater diameter is 300 m at the floor, but the fringing talus could conceal on orifice as wide as 350 m or, alternatively, the steep walls could taper inward beneath the crater fill to a still narrower conduit. Assuming a vent radius of 150 m and a pre-eruptive magmatic water content of 4–5 wt% (for hornblende-bearing silicic magma; Rutherford and Devine 1988), the models of Sparks (1986), Carey and Sparks (1986), and Wilson and Walker (1987) were applied to the isopleth data of Figure 8 for 0.5-to-5-cm lithics and 5-to-20-cm pumice clasts. Results are given in Table 3. Still coarser ejecta yield results inconsistent with these, probably because of ballistic behavior unrepresentative of fallout from high parts of the convecting column and umbrella cloud. The models yield peak mass eruption rates in the range $0.9–2.5 \times 10^8$ kg/s and maximum column heights between 25 and 32 km (Table 3), in agreement with an estimate of 27–30 km based on a photograph taken 5 hours into the plinian eruptive phase (Bobillier 1934).The peak intensity (mass eruption rate) thus calculated also agrees well with the observational record; if the condensed volume of 4.05 km^3 having a magma density of 2.4 g/cm^3 were released in 18 hours, the average discharge rate was 1.5×10^8 kg/s. Of 45 plinian eruptions for which intensities were estimated by Carey and Sigurdsson (1989) using similar methods, about half had similar or greater mass eruption rates than Quizapu.

On the other hand, the nominal wind velocity of at least 30–35 m/s obtained by the isopleth methods of Carey and Sparks (1986) is in poor accord with the apparent ash transport rate of 19–20 m/s observed between the plinian outbreak (~1200) and the onset of

ashfall (~0400) at Buenos Aires and La Plata (1125–1160 km in 16 hours). Owing to nighttime darkness in eastern Argentina, however, the lag time between arrival of the ashcloud overhead and settling of the fine distal ash to ground level was not established. Neither can we account easily for the northwesterly expansion of the plume on the morning of the second day (11 April), while vigorous eastward transport was still taking place along the main dispersal axis. Fine ash fell as far as 320 km NNW of source (to Quintero), but none at all fell in Talca, only 85 km WNW of source. Variations of wind velocity with altitude and time are likely causes (as during several 1980 eruptions of Mount St. Helens; Sarna-Wojcicki 1981), but we know of no relevant wind data for 1932.

The high H_2O content expected for hornblende-dacite magma (e.g., Rutherford and Devine 1988; Merzbacher and Eggler 1984) would promote both high exit velocity and low bulk density of the eruptive jet, enhancing entrainment of air and vigorous convective column ascent. For any reasonable choices of vent radius, mass eruption rate (Table 3), and water content (3–6 wt% H_2O), the Quizapu column would have remained remote from the threshold between collapsing and stably convecting columns as given in the updated column model of Wilson and Walker (1987). Only during extinction of the plinian column was a pyroclastic flow as voluminous as 0.01 km^3 generated. The two or three synplinian ignimbrites observed are lithic-rich, swale-confined, only 0.3–2 m thick, and <0.001 km^3 in volume. They may reflect the effects of vent-wall roughness or of local wall-spalling events on the velocity and load at the jet margins, processes that caused no perturbation of the main central part of an evidently very steady column.

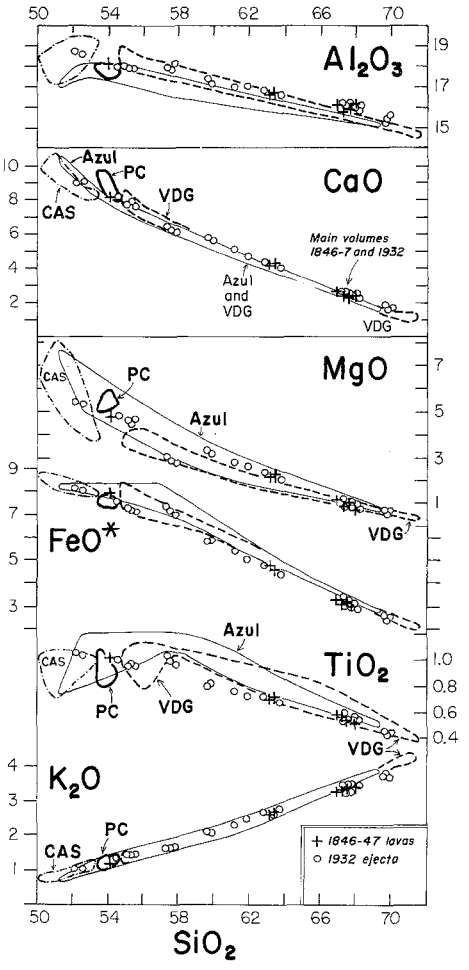

Fig. 12. Major-element compositions of 1846–47 lavas (+) and 1932 ejecta (O) from Table 4. More than 95% of the material in each eruptive sequence is 67–68% SiO_2 dacite. Also shown are fields for the Casitas shield (CAS; $n=8$), Cerro Azul ($n=16$), Volcán Descabezado Grande (VDG, dashed enclosure; $n=14$), and six mafic peripheral cones (PC; $n=9$). For clarity, medial part of dashed enclosure for VDG is omitted in panels where it coincides with the line enclosing the Azul field

1846 vs 1932: Petrologic data bearing on the contrasting modes of eruption

The Quizapu eruptions of 1846–47 and 1932 released ~5 km^3 and ~4 km^3, respectively, of nearly identical magma, but the first was effusive and the second plinian. The 1932 vent coincided with at least part of the 1846 vent (which, if fissural, could conceivably extend slightly farther NNE beneath the pumice cover). The petrologic data that follow are provided primarily to illustrate how closely similar the magmas were and to assess the basis for the contrasting styles of eruptions separated by only 86 years.

Bulk Composition

Major-element compositions of 24 samples of 1932 ejecta and 7 of 1846–47 lavas are given in Table 4 and plotted in Figure 12. Six blocks of 1932 dacite pumice, taken from base to top of the deposit and including a post-plinian breadcrusted block on the crater rim, fall in the narrow range 67.4–68.1% SiO_2. Samples from four different 1846–47 lava flows yield 67.0–68.0% SiO_2, essentially indistinguishable from the 1932 dacite (Fig. 12). These dacites make up more than 95% (perhaps 98%) of the material erupted in each episode.

Banded pumice occurs sparsely throughout the 1932 plinian sequence (and is abundant in the initial scoria and in the brown band). Macroscopically homogeneous basaltic to andesitic scoriae (52.1–63.7% SiO_2) are also present, sparsely in the plinian deposit and abundantly in the initial and terminal scoria falls. In the 1846–47 lavas, mafic and intermediate magmatic inclusions appear to represent similar magma that had mixed in varying degrees with the host dacite; the three samples analyzed plot colinearly with 1932 scoriae (Fig. 12).

Three blocks of the frothy rhyodacite pumice of 1932 taken from widely separated locations yielded essentially identical compositions at $69.8 \pm 0.05\%$ SiO_2 (Table 4). Such materials is scattered sparsely throughout the plinian deposit, of which it may make up ~0.5%. Nothing equivalent has been found in the

Table 4. Major-element analyses for Quizapu[a]

1932 Ejecta	SiO_2	TiO_2	Al_2O_3	FeO[a]	MnO	MgO	CaO	Na_2O	K_2O	P_2O_5	H_2O	Original total[a]
Q-1	57.4	1.03	17.95	7.36	0.14	3.05	6.49	4.30	1.59	0.32	0.5	99.3
Q-2	69.8	0.43	15.44	2.42	0.07	0.68	1.81	5.16	3.72	0.10	0.85	99.5
Q-3	63.7	0.68	16.66	4.40	0.09	2.09	4.09	4.92	2.72	0.20	0.74	100.2
Q-3a	62.95	0.71	16.80	4.74	0.10	2.36	4.41	4.75	2.60	0.18	0.9	98.8
Q-4	67.9	0.55	15.95	3.09	0.08	0.89	2.38	5.25	3.38	0.14	0.97	98.3
Q-5	67.9	0.56	15.89	3.05	0.08	0.96	2.41	5.28	3.36	0.10	0.88	99.3
Q-6	68.1	0.56	16.07	2.89	0.08	0.89	2.39	5.16	3.35	0.11	0.73	98.8
Q-7	55.4	0.95	17.97	7.19	0.12	4.67	7.82	3.86	1.41	0.20	0.11	100.9
Q-8	67.7	0.55	16.06	3.09	0.08	0.93	2.42	5.34	3.31	0.15	0.40	99.5
Q-9	59.65	0.80	17.39	5.82	0.11	3.29	5.90	4.40	2.07	0.19	0.27	100.1
Q-10	67.4	0.57	16.05	3.24	0.08	1.10	2.65	5.16	3.23	0.10	0.67	99.5
Q-16	54.5	1.00	17.95	7.57	0.13	4.86	8.26	3.80	1.29	0.22	0.2	100.5
Q-17	52.6	1.04	18.62	8.03	0.13	5.35	9.12	3.55	0.98	0.23	<0.1	100.7
Q-18	55.3	0.96	17.95	7.21	0.12	4.50	7.96	3.92	1.42	0.22	0.2	99.9
Q-21	67.8	0.56	15.86	3.11	0.08	0.94	2.52	5.31	3.29	0.16	0.8	98.9
Q-81	69.85	0.44	15.54	2.47	0.07	0.65	1.81	5.08	3.59	0.10	0.79	100.1
Q-82	69.8	0.44	15.27	2.55	0.07	0.71	1.86	5.16	3.66	0.12	0.86	98.7
Q-85	55.3	0.94	17.95	7.20	0.12	4.61	7.78	4.11	1.42	0.20	0.17	99.9
Q-89	52.1	1.05	18.71	8.11	0.13	5.43	9.01	3.82	0.99	0.22	0.15	99.6
Q-91	61.9	0.73	17.06	5.03	0.11	2.63	4.83	4.75	2.42	0.16	0.36	99.0
Q-92	59.8	0.82	17.17	5.87	0.11	3.21	5.72	4.62	2.05	0.18	0.24	99.7
Q-93	57.8	0.96	18.14	7.00	0.13	2.81	6.21	4.61	1.60	0.30	0.33	99.9
Q-94	61.2	0.76	16.99	5.37	0.11	2.80	5.20	4.80	2.24	0.18	0.25	100.1
Q-95	57.6	0.98	17.86	7.17	0.13	2.91	6.36	4.72	1.59	0.30	0.33	99.8
1846–47 Lavas												
Q-22	68.0	0.52	16.03	2.97	0.08	0.94	2.42	5.15	3.33	0.16	0.2	100.8
Q-34	67.4	0.56	16.02	3.19	0.08	1.03	2.52	5.33	3.30	0.16	0.2	99.1
Q-35	67.0	0.58	16.06	3.32	0.09	1.12	2.67	5.30	3.26	0.16	0.1	99.5
Q-52	67.3	0.58	15.93	3.28	0.08	1.01	2.61	5.36	3.27	0.16	0.3	99.7
Q-59a	63.15	0.71	16.61	4.74	0.10	2.19	4.39	4.94	2.58	0.18	<0.1	99.9
Q-59b	63.4	0.70	16.66	4.66	0.10	2.21	4.33	4.69	2.65	0.19	0.2	99.6
Q-59c	54.1	1.01	18.18	7.99	0.13	4.80	8.23	3.75	1.15	0.23	0.1	99.8

[a] The ten major oxides are normalized to H_2O-free totals of 99.6 wt% (allowing ~0.4 wt% for trace oxides and halogens). The H_2O column lists determinations of H_2O^+ (2 decimal figures) or LOI (1 decimal figure). "Original Total" is the anhydrous sum of the ten oxides with total iron as Fe_2O_3. The FeO[a] values listed were recalculated (before normalization) on the assumption that 25% of the Fe in the magma had been ferric. Determinations by XRF in USGS laboratory in Lakewood, Colorado, supervised by J. Taggart. H_2O determinations by T. Fries and S. Pribble

1846–47 lavas, but it would be hard to identify and a thorough search has not been completed.

Concentrations and ratios of several incompatible trace elements are plotted in Fig. 13 for most of the samples represented in Fig. 12. The main feature of interest here is that in all respects the compositions of 1846–47 and 1932 dacites are virtually identical (at 101–111 ppm Rb). This suggests that the magmas were batches sequentially tapped from the same reservoir and probably, in a stricter sense, even from the same "chamber".

An additional important feature shown in Fig. 13 is the range of trace-element ratios (Ba/Ta, Ba/La, La/Yb, Zr/Y, Zr/Rb, and Zr/Hf) among ejecta that were erupted concurrently within an interval of several hours in 1932. This illustrates that coherent gradients in such ratios can exist within a crustal magma reservoir as modest as that beneath Quizapu. Such gradients (even for the mafic end of the suite) indicate that these ratios are influenced by crustal processes and should be interpreted as geochemical indicators of mantle sources only with appropriate caution.

Although most of the 1932 ejecta were fairly uniform dacite, the full range of compositions (52–70% of SiO_2) released on 10–11 April 1932 makes this one of the most extensively zoned eruptions known.

Aeolian fractionation

The progressive loss of crystals (and lithics and mafic shards) downwind from vent, producing bulk ash compositions increasingly evolved, was explicitly discussed and documented by Kittl (1933), but the term "aeolian differentiation" was apparently coined by Larsson (1937) in the course of elaborating Kittl's data. The Quizapu fallout is thus sometimes cited as a type example of the process, but the results have never really been well documented. Ironically, the enormously wide range of magmatic compositions (52–70% SiO_2) erupted in 1932 complicates such an analysis substantially. Kittl recognized a range of pumice compositions in the field, but he failed to analyze the dominant pumice (67–68% SiO_2; Fig. 12), and his chemical analyses are not satis-

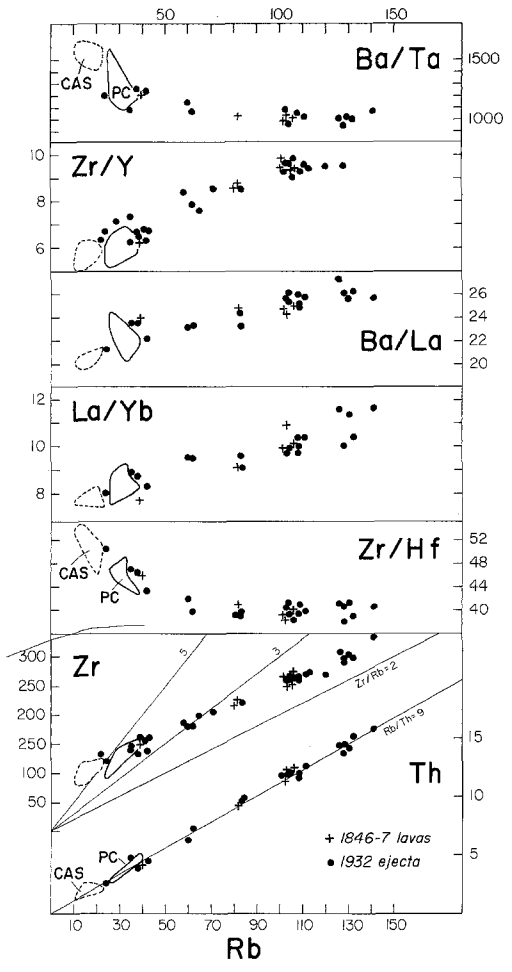

Fig. 13. Selected trace-element concentrations and ratios for 1846–47 lavas (+) and 1932 ejecta (●). Also shown are a field for the Casitas shield (CAS) and another for mafic samples (<55% SiO_2) from Cerro Azul and its peripheral cones (PC; cf. Fig. 12). Unpublished USGS data (Hildreth and Drake, in prep.); Rb, Y, Zr, Ba by energy-dispersive XRF, others by INAA. Three samples having ≥130 ppm Rb are glasses separated from dacites. Note that Rb-Th line projects through the origin

factory by present-day standards. The analyses of bulk ash by Kreutz and Jurek (1932) and Larsson (1937) from 1125 km and 810 km downwind, respectively, are apparently better. They gave 70.05% and 70.4% SiO_2 for ash still having 5–7 wt% crystals, values in reasonable accord with microprobe determinations of 71–72.5% SiO_2 for the glass phase in the dacite pumice (all values normalized dry to 100%). In addition to 5–8 wt% crystals, the fallout in eastern Argentina also retains trace fractions of shards derived from mafic scoriae and from accidental lithic material.

Mineralogy

The dominant dacites of the two eruptions contain 15–19% total phenocrysts (Table 5) and have similar relative abundances of plagioclase > opx ≈ hornblende ≥ titanomagnetite ≫ ilmenite ≈ cpx > apatite > sulfide blebs. Zircon, sanidine, and quartz were sought but not found. The only differences noted in phenocryst abundances are the apparently greater content of titanomagnetite in 1932 dacite and the consistently greater amount of (invariably sparse) cpx in 1846–47 dacite.

The pre-, syn-, and post-plinian scoriae additionally contain olivine (Fig.14), as do many or all mafic inclusions in the 1846–47 lavas. Most samples having <63% SiO_2 lack hornblende; three samples having 59.6, 63.1, and 63.7% SiO_2 contain both olivine and hornblende and are presumed to be of mixed parentage. The 1932 rhyodacite pumice has fewer than half as many phenocrysts as the dacite (Table 5) but has more cpx; it too lacks quartz and sanidine. In separates from 1932 fallout in Argentina, Kittl (1933) reported sparse and tiny fragments of what he tentatively identified optically as sanidine. Neither in thin section nor by microprobe have we found any sanidine, but granitoid xenoliths and K-feldspars liberated from them are present sparsely among the 1932 ejecta.

Electron microprobe analyses of 10–30 grains of most species in each of several 1846–47 and 1932 samples are summarized in Figures 14 and 15. Phenocryst compositions in the dominant dacites are almost identical. (1) The range of zoning in plagioclase from the dacites of each eruption is identical at An_{25-50}; in 1932 rhyodacite pumice the range is An_{23-39} (Fig. 14). Normal and reverse zoning coexist in all dacite samples investigated, but there is a greater incidence of reverse zoning in 1846–47 dacites, perhaps owing to the ubiquity of mafic magmatic inclusions. (2) Augites are identical and almost unzoned (at En_{44} Fs_{13} Wo_{43}) in the 1932 and 1846–47 dacites. (3) The range of zoning in hypersthenes is $En_{69.5-64}$ in 1846–47 dacites and trivially wider at $En_{69.5-63}$ in 1932 dacites. In both eruptions the dacitic hypersthenes have low CaO ($Wo_{2.0-2.6}$), modest Al_2O_3 (Fig. 15), and reverse zoning prevalent over normal. In 1932 scoriae and 1846–47 mafic inclusions, both pyroxenes are compositionally distinct from those in the dacites (Fig. 14). (4) Amphiboles are calcic (10.3–11.9% CaO, 0.5–0.8% K_2O) and show considerable compositional ranges that are more complex than simple core-to-rim zoning; nonetheless, Figure 15 shows that there is wholesale compositional overlap between the 1846–47 and 1932 hornblendes. Halogen contents are modest, showing limited unsystematic zoning (F=0.28–0.50; Cl=0.03–0.08 wt%) and essentially identical averages (0.34–0.36 F; 0.06–0.07 Cl) for numerous amphiboles from the two eruptions.

The only significant (?) differences defined by microprobe between phenocrysts in 1932 and 1846–47 dacites are the apparently wider range of Fe_2O_3 in 1932 plagioclase and the slightly lower contents of MnO in 1846–47 hypersthene (Fig. 15).

Magma temperatures

Coexisting ilmenite and titanomagnetite are ubiquitous in the dacites and rhyodacite, but ilmenite is sparse or absent in the andesites and basalts. Contiguous mineral pairs were located in a few instances, but generally 10–

Table 5. Phenocryst contents of Quizapu samples

	Plag	Opx	Amph	Mt	Cpx	Ol	Total
Mineral separations (wt%)							
1932 Rhyodacite Pumice							
Q-2	4.8	1.45	0.50	0.56	0.08	0	7.4
Q-81	4.2	1.21	0.57	1.01	0.04	0	7.0
1932 Dacie Pumice							
Q-4	11.1	1.55	1.69	1.38	tr	0	15.7
Q-5	11.2	1.50	1.37	1.59	0	0	15.7
Q-6	11.9	1.03	1.69	1.22	0	0	15.8
Q-10	11.4	2.32	2.80	1.28	0.01	0	17.8
Q-12	11.3	1.11	1.58	1.52	0	0	15.5
1932 Andesite Scoria Bomb							
Q-7 (terminal)	~19	0	0	[a]	0	~7	~26
Point counts (vol%)							
1932 Dacite Bombs							
Q-6	12.7	0.3	2.0	0.9	—	—	15.9
Q-8	13.6	0.3	2.1	0.8	—	—	16.8
1932 Andesite Scoria Bombs							
Q-9 (terminal)	20.3	0.2	1.1	0.3[a]	—	3.6	25.5
Q-16 (terminal)	22.9	0.2	—	0.1[a]	—	2.5	25.7
Q-18 (terminal)	20.9	—	—	[a]	—	6.1	27.0
Q-93 (initial)	33.8	6.4	tr	2.4	3.3	—	45.9
1932 Basaltic Scoria Bombs							
Q-17 (terminal)	30.7	—	—	[a]	—	5.5	36.2
Q-89 (terminal)	30.5	—	—	[a]	—	6.4	36.9
1846–47 Dacite Lava							
Q-22	12.0	1.5	1.5	[a]	tr	—	15.0
Q-34	13.3	1.7	1.7	0.3[a]	tr	—	17.0
Q-35	15.6	1.9	1.4	0.7[a]	tr	—	19.6
Q-52	14.8	1.0	1.4	[a]	0.1	—	17.3
Prehistoric Rhodacite Lava (from Cerro Azul)							
Q-36	2.4	0.3	0	1.7	0.1	0.2[b]	4.7

Quantitative mineral separations can provide much more precise modal data for vesicular glassy rocks than can point counting, but satisfactory separation is not feasible for devitrified samples. Merely incipient devitrification caused difficulty with Q-7, a vesicular scoria bomb. Point-count data (in volume %) are based on 1100–1800 points per thin section

[a] Magnetite abundant in groundmass but not feasible to point count with precision

[b] Olivine in Q-36 was apparently released from mafic magmatic inclusions common in the host lava

20 isolated grains of each mineral were analyzed from a sample, any subpopulations averaged separately, and equilibrium pairs identified by the Mg/Mn partitioning criterion of Bacon and Hirschmann (1988). Values of T and fO_2 obtained via the procedure of Stormer (1983) and the solution model of Andersen and Lindsley (1988) are plotted in Figure 16.

Six samples of 1932 dacite pumice yielded 863°–870° C and a seventh gave 855° C. Five samples of 1846–47 dacite lavas show a wider range of 837–874° C, completely overlapping the values for 1932 dacites.

Two rhyodacite pumice blocks gave 860° and 865° C, essentially identical to coeruptive dacite. This suggests that the minor, phenocryst-poorer (Table 5) rhyodacite component of the 1932 magma had been situated in a contiguous, thermally equilibrated but possibly water-richer, zone or apophysis of the dacite reservoir. The rhyodacite magma, however, was apparently not located close to the conduit, at least initially, because it bled sparingly into the magma column throughout the plinian interval rather than being preferentially flushed early in the eruption.

Only a single sample (61.2% SiO_2, >45 wt% phenocrysts) of initial scoria has so far yielded oxide pairs in apparent equilibrium. They gave surprisingly low temperatures of 815° and 819° C (Fig. 16) on the basis of two slightly different titanomagnetite compositions. Perhaps these temperatures are realistic for the crystal-rich, probably water-rich, silicic andesite that opened the eruption. If so, it is unlikely that this magma had been stored contiguously with the dominant (hotter) dacite magma, with which it mingled syneruptively to produce the banded pumice so abundant in the opening phase.

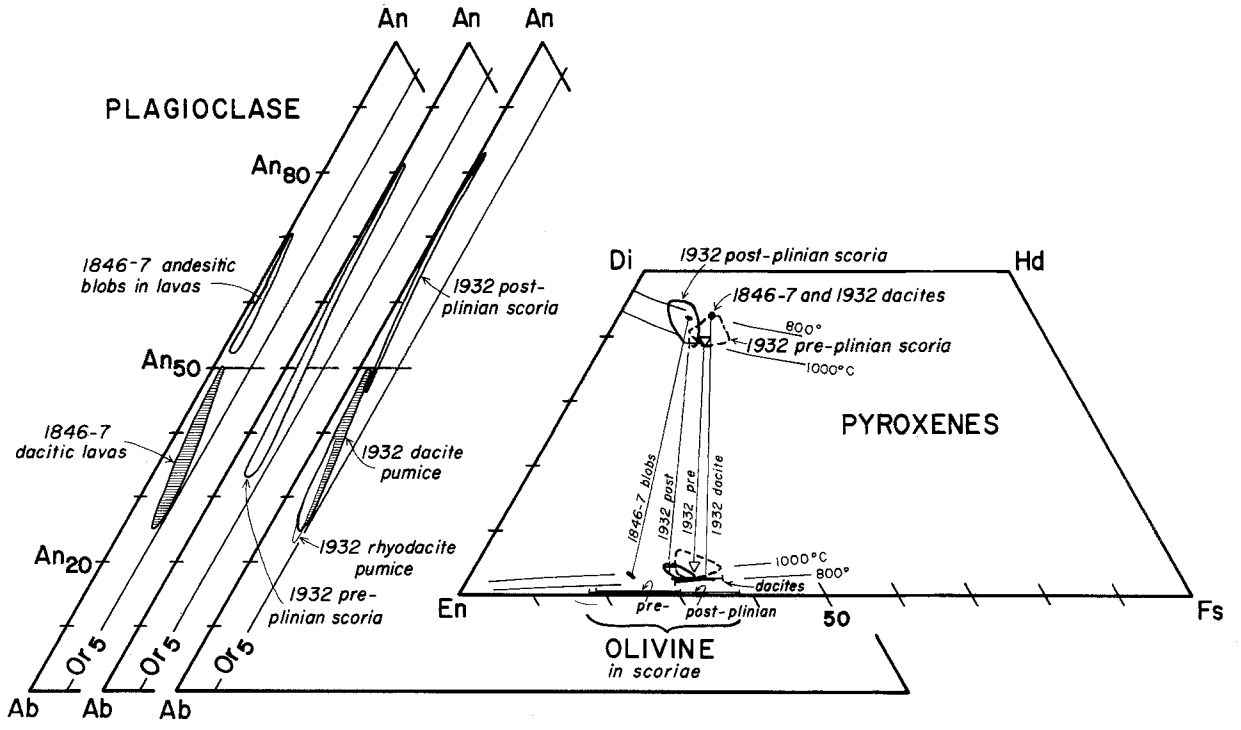

Fig. 14. Compositional ranges of plagioclase, olivine, and pyroxenes in 1846–47 lavas and 1932 ejecta. Plagioclase range is virtually identical (An_{50-25}) in the dominant dacites of the two eruptions; 1932 rhyodacite only slightly extends that range. The hypersthene range in 1846–47 dacite lavas (*bar*) is overlapped and marginally extended by that of 1932 dacite pumice (*fine line with terminal ticks*). *Tie lines* connect coexisting cpx and opx in selected samples from each field shown. One-atmosphere isotherms are from Lindsley (1983). Electron microprobe analyses by W. Hildreth using ARL/SEMQ instrument at Menlo Park

Radiogenic-isotope compositions

Only narrow ranges of Sr, Nd, and Pb isotope ratios have been found for eruptive products of the Azul-Descabezado cluster (Hildreth and Moorbath 1988), and if any real shifts took place within the Quizapu subsystem between 1846–47 and 1932, they are near the limits of analytical resolution. $^{143}Nd/^{144}/Nd$ values are nearly constant for the whole cluster at 0.51280 ± 2 ($\varepsilon_{Nd} = +3.0$ to $+3.5$), and within analytical error all values for Quizapu samples overlap. Pb-isotope ratios vary little and, within the errors ($\pm 0.1\%$), values for 1846–47 and 1932 products of Quizapu are indistinguishable (Fig. 17).

Among the 1932 ejecta, there is a clear tendency for more evolved samples (higher SiO_2, lower Sr) to have less radiogenic $^{87}Sr/^{86}Sr$ values (Fig. 17). The Sr data for two 1846–47 dacite lavas plot near but significantly displaced from data for 1932 dacite and rhyodacite pumice; they nonetheless fall along the trend between silicic and mafic members of the 1932 suite. Because the full Sr-isotopic range of the 1846–47 lavas is unlikely to be represented by only two samples, it remains uncertain whether any Sr-isotopic change took place in the magma reservoir during the 86 years between eruptions.

The range and trend of the Sr data for Quizapu require mixing between more radiogenic (>0.7040) basaltic magma and less radiogenic (<0.7039) silicic magma. The latter could have evolved from a mafic parent like some of the peripheral-cone or Casitas shield magmas (Fig. 17) or by assimilation of unradiogenic wallrocks – conceivably mafic intrusions related to the 0.34-Ma Casitas shield. Although rare partially melted fragments of the Invernada granitoid pluton (Fig. 2) occur among the 1932 ejecta, their Sr-isotopic ratios are too high (0.7039–0.7046; Hildreth and Moorbath 1988) to provide the unradiogenic assimilant necessary. On the other hand, the relatively low Pb-isotopic ratios for Quizapu (Fig. 17) require a crustal input containing Pb less radiogenic than in any older unit of the Azul-Descabezado system yet analyzed. Whatever the unradiogenic contribution may be, the fact that the Quizapu Sr-isotope trend crosscuts that for Holocene and older products of Azul and Descabezado (Fig. 17) suggests that establishment of the (presumably upper-crustal) assimilation regime was very recent – probably during growth of the dacite magma body that first erupted in 1846.

Stable-isotope compositions and magmatic degassing

$\delta^{18}O$ and δD data are given in Table 6 and Fig. 18 for 1846–47 and 1932 dacites and for mafic products of these and earlier eruptions. Since the 1932 pumice is variably hydrated and the 1846–47 lavas degassed to H_2O contents of <0.3 wt% (Table 4), and because ejected fragments of massive conduit-lining vitrophyre chilled at depth (Taylor et al. 1983; Newman et al. 1988) have not been found at Quizapu, hornblende and plagioclase phenocryst separates were analyzed in or-

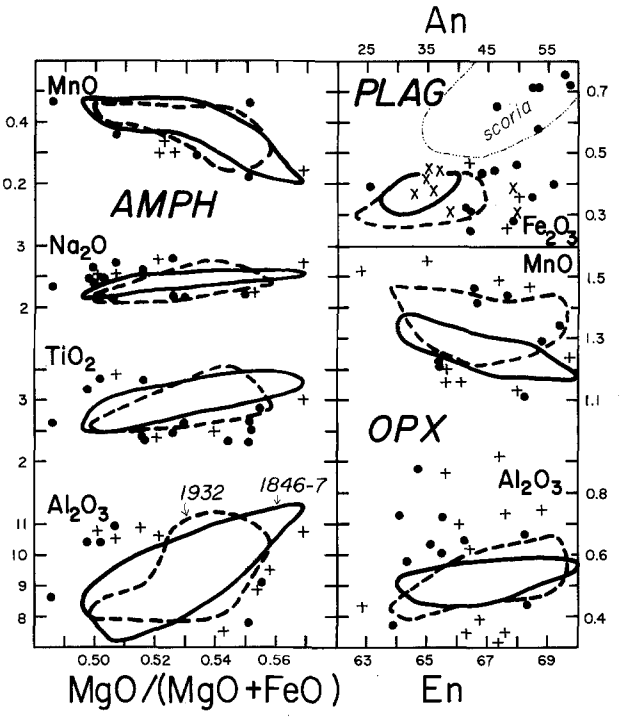

Fig. 15. Ranges of selected minor elements in amphibole, hypersthene, and plagioclase from 1846–47 dacite lavas (*solid lines*) and 1932 dacite pumice (*dashed lines*). For each mineral, the fields represent >60 1846–47 crystals and >100 1932 crystals, from several samples. Compositions (*zones within crystals*) that fall outside the dense clusters of data are plotted individually; *dots* for 1846–47, *crosses* for 1932. Also shown in the plagioclase panel is the evolved end of a field for andesitic scoria; X's represent grains or overgrowth zones in pre- and syn-plinian andesite that had mingled with dacite magma

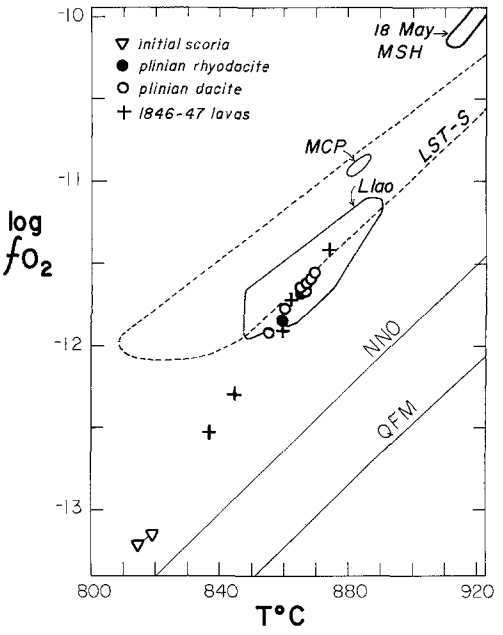

Fig. 16. Temperature and fO_2 values for coexisting titanomagnetite and ilmenite in 1846–47 lavas (+) and 1932 ejecta (▽ = crystal-rich initial scoria; ● = plinian rhyodacite; ○ = plinian dacite). Microprobe analyses recalculated by procedure of Stormer (1983); T-fO_2 values determined by the solution model of Andersen and Lindsley (1988). For samples having mixed subpopulations, equilibrium pairs were identified by the Mg/Mn partitioning criterion of Bacon and Hirschmann (1988). Also shown are fields for other selected hornblende dacites and rhyodacites: *MCP* and *Llao* are Mazama climactic pumice and Llao Rock rhyodacites of Druitt and Bacon (1989); *LST-S* is ignimbrite cooling unit S of the Loma Seca Tuff (erupted 25 km NE of Quizapu; Grunder and Mahood 1988); *MSH* is 18 May 1980 pumice from Mount St. Helens (Rutherford and Devine 1988). Buffer curves; *NNO* after Huebner and Sato (1970); *QFM* after Frost et al. (1988)

der to estimate pre-eruptive $\delta^{18}O$ and δD values of the magmas. In parts of the lavas that were oxidized or underwent extensive groundmass crystallization, hornblende phenocrysts developed opaque, oxidized rims. Such material was avoided, and pristine unrimmed hornblende was separated from fresh 1846–47 lava-margin vitrophyre and from 1932 pumice.

For the dominant dacites of the two eruptions, $\delta^{18}O_{plag}$ values are similar (5.55 ± 0.25‰). As $\delta^{18}O_{melt}$ values are expected to be only 0.1–0.3‰ heavier, the average for the dacite magma was probably in the range 5.5–5.9‰, which is slightly lighter than most of the mafic products of these and older eruptions of the Quizapu-Azul-Casitas system (Fig. 18). Because fractionation of plag + px + oxides ± hb ± ol could only have raised the $\delta^{18}O$ value of evolving magmas, this apparent shift to lighter values implies assimilation of low-^{18}O roof rocks (and perhaps their interstitial meteoric water) by the dacite magmas (cf. Grunder 1987; Bacon et al. 1989) – in accord with the $^{87}Sr/^{86}Sr$ and trace-element evidence for assimilation cited earlier (Figs. 13, 17). Partially fused xenoliths (like those studied by Bacon et al. 1989) are rare at Quizapu, but a frothy bomb of extensively fused granite (75.5% SiO_2) among the 1932 ejecta on the crater rim gave a bulk $\delta^{18}O$ value of −1.8‰ (Table 6; Q-19). As this xenolith and others define a 7-Ma Rb-Sr isochron (Hildreth and Moorbath

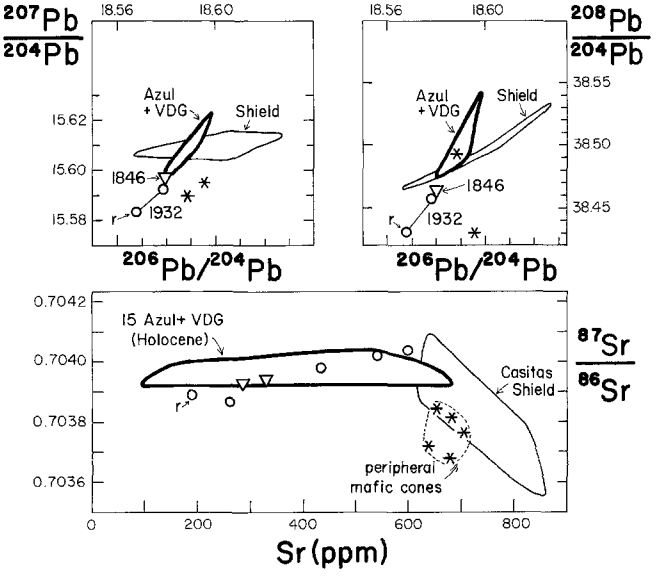

Fig. 17. Pb and Sr isotope data for 1846–47 lava (▽) and 1932 ejecta (○; *r* = rhyodacite pumice Q-2) compared to fields for the (largely Holocene) products of Cerro Azul and Volcán Descabezado Grande (VDG) and for the 0.34-Ma Casitas shield (Fig. 2). *Stars* are peripheral mafic cones of Holocene age. Data from Hildreth and Moorbath (1988)

Table 6. Stable isotope data for Quizapu

	Whole-rock SiO_2	$\delta^{18}O$			δD	
		Plag	Hb	WR	Hb	Other
1846-7 lavas						
Q-22	68.0	5.5	4.6		−80	
Q-34	67.4	5.3	4.6	5.5	−73	−111 (glass)
Q-35	67.0	5.5				
Q-52	67.3	5.5			−79	
Q-59i	54.1	5.9				
1932 ejecta						
Q-2	69.8	5.4	4.7		−59, −60	
Q-3	63.7	5.5				
Q-4	67.9	5.6	4.6		−36, −38	
Q-5	67.9	5.7			−65	
Q-6	68.1	5.8	4.6		−27	
Q-10	67.4	5.4			−64	
Q-81	69.9	5.6			−60	
Q-7	55.4			6.1		
Q-9	59.7			6.1		
Q-16	54.5			5.9		
Q-17	52.5			5.9		
Granitic xenolith (partially melted)						
Q-19	75.5			−1.8		− 93 (WR)
Snow at Quizapu						
W-16	0.0			−8.4		− 60 (Snow)

Whole-rock values of SiO_2 in wt%, with analytical totals recalculated to 100% H_2O-free; data from Table 4. Stable-isotope data are given in permil relative to SMOW; W. Hildreth, L. Adami, C. J. Janik, and L. D. White, analysts. Replicate analyses routinely give a $\delta^{18}O$ value of 9.6 permil for quartz standard NBS-28 and indicate typical precision of ±0.15 permil for $\delta^{18}O$ and ±2 permil for δD

1988 and unpubl. data), they were evidently torn from the subjacent Invernada pluton (Fig. 2), which has been K-Ar dated at 7 Ma (Drake 1976). The roof of the 1932 dacite magma body apparently lay within the pluton, some parts of which had been depleted in ^{18}O and D by hydrothermal alteration prior to partial fusion. The scarcity of such altered material among the ejecta and in surrounding outcrops of the pluton (Fig. 2), however, suggests that the hydrothermal focus may have been restricted to the vicinity of the 1846–47 conduit (or to older conduits of Cerro Azul).

δD_{hb} determinations for hornblende from 1932 pumice blocks yield a range of values (−27 to −65‰) that is consistently heavier than that for chemically similar, unoxidized hornblende from glassy 1846–47 lavas (−73 to −80‰; Fig. 18). This apparent difference in D/H is the only significant compositional distinction identified between the 1846–47 and 1932 dacites. Assuming that the values reflect magmatic D/H fractionations rather than isotopic changes that took place in hornblende phenocrysts during the one-day eruption, it seems likely that *pre-eruptive* degassing had produced a range of δD values within the dacite magma reservoir prior to the 1932 plinian outburst. Moreover, the 5-km^3 batch of dacite magma extruded in 1846–47 had evidently degassed even more extensively prior to emplacement than had the 1932 batch.

These data are not straightforwardly comparable with those of Taylor et al. (1983) and Newman et al. (1988), who investigated eruptive degassing of silicic magma by determining δD and H_2O contents of ejected fragments of quenched conduit-lining obsidian. The euhedral hornblende phenocrysts analyzed here had crystallized before the eruptions began, and the main uncertainty concerns how much of their deuterium loss took place during strictly pre-eruptive degassing and how much could have taken place during sluggish syneruptive ascent that culminated in effusion in 1846 and in explosive fragmentation in 1932.

Nonetheless, the large vapor-melt D/H fractionations ($\Delta D_{vapor\text{-}melt} = +10$ to +40‰ at 850° C in H_2O-rich silicic magmas) identified by Newman et al. (1988) and Dobson et al. (1989) make a pre-eruptive equivalent of the quasi-closed-system progressive-degassing model of Newman et al. (1988) our preferred mechanism for lowering δD_{hb} by as much as 40‰ (Fig. 18) in the course of passively exsolving a few wt% of H_2O. The 1846–47 batch had evidently degassed sufficiently at deeper levels that during final ascent the remaining magmatic water was released without significant generation of tephra. Nonvesicular glass separated from an 1846–47 lava gave $\delta D = -111$‰ (Table 6), illustrating the advanced deuterium loss (in conjunction with a negligible shift in $\delta^{18}O$) that occurs when magmatic degassing essentially goes to completion during extrusion at atmospheric pressure.

An alternative scenario, that contrasting amounts of assimilation of water-rich low-D roof rocks might have

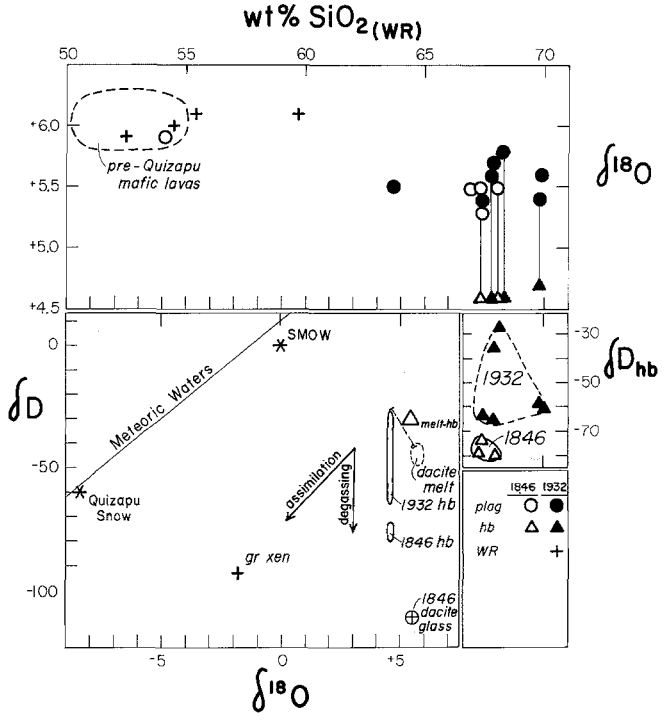

Fig. 18. Values of $\delta^{18}O$ and δD (in hornblende) in permil relative to SMOW (standard mean ocean water) for 1846–47 lavas and 1932 ejecta, plotted against wt% SiO_2. Data in Tables 4 and 6. Symbols are explained in inset. *Field at upper left* encloses whole-rock $\delta^{18}O$ values for mafic lavas of Cerro Azul, the peripheral cones, and the Casitas shield (Fig. 2). Lower-left panel gives the $\delta^{18}O$-δD field expected for pre-eruptive Quizapu dacite magma, based on 850° C fractionations anticipated among vapor, melt, hornblende, and plagioclase (Dobson et al. 1989; Suzuoki and Epstein 1976; Taylor and Sheppard 1986). Also plotted are isotopic values for snow adjacent to Quizapu crater, a partially molten granitic xenolith in 1932 fallout, a glass separate from degassed 1846 lava (Q-34), the meteoric-water line of Craig (1961), and trends anticipated for magmatic degassing and for assimilation of hydrothermally altered roof rocks

controlled the magmatic D/H relations, appears to be ruled out because (1) it was the lower-δD dacite that erupted effusively, (2) there was no difference in $\delta^{18}O$, and (3) there was no significant difference in fO_2 or temperature (Fig. 16) between the mineralogically and compositionally equivalent batches of 1846–47 and 1932. The stable-isotope basis of this argument is illustrated in Figure 18.

So, how did 5 km^3 of hornblende-dacite magma degas passively? If Quizapu dacite had once contained 4–5 wt% H_2O, like the hb-px-plag dacites of similar or slightly higher temperature (Fig. 16) studied at Mount St. Helens (Rutherford and Devine 1988) and Mount Mazama (Bacon et al. 1988), then $>5\times10^{11}$ kg of H_2O must have exsolved passively from the 5 km^3 of magma emplaced effusively in 1846–47. As liquid water, this would be volumetrically similar ($\sim$0.5 km^3) to the 5-km-long Laguna Invernada (Fig. 2). However, no fumaroles had been reported during centuries of observation, and generations of arrieros had seasonally driven their livestock over the subsequent site of Quizapu without mentioning any fumaroles or nearby hot springs (Domeyko 1903). Similarly, after dying out on the 1846–47 lavas (prior to 1873), fumaroles were said to have been absent until the initiation of explosive activity around 1907 (Fuenzalida 1943). Had some of the magmatic water escaped pre-eruptively from the saturated top of the magma body or during upward dike intrusion, it must have been dispersed in deep aquifiers without producing any obvious hydrothermal manifestations nearby.

Discussion and implications

The 1846–47 lavas were the first products of the Cerro Azul center to contain hornblende. A spectrum of basalts through pyroxene dacites had built the main edifice, and the youngest pre-Quizapu product (a spatterfed lava flow from the summit vent only 1.5 km south of Quizapu) was a phenocryst-poor, hornblende-free, pyroxene rhyodacite (Q-36; Table 5) that is chemically *more* evolved (69.2% SiO_2) than 1846–47 dacite. As the flow appears to be of post-Neoglacial age, the evolution of silicic magma sufficiently cool and hydrous to crystallize hornblende may have taken place as little as a few centuries before 1846. Growth of the silicic magma body within a wall-rock envelope of hb-bi granodiorite (Invernada pluton) may have helped by providing a hydrous assimilant.

The stable hornblende phenocrysts in the Quizapu dacites indicate that the melt had once contained at least several wt% H_2O (Merzbacher and Eggler 1984). Pre-eruptive loss of sufficient water to avoid near-surface explosive fragmentation apparently requires considerable depressurization of the magma after it attained water saturation. A thermal pulse caused by injection of mafic magma and the attendant convection (evident in its dispersal as chilled mafic inclusions throughout the voluminous 1846–47 dacite) may well have contributed to promoting vapor loss, but the main process had to be decompression. Advance of the magma reservoir itself by diking, stoping, melting, or deforming its roof might account for some of the apparent ascent, but the lack of subsidence in response to the Quizapu eruptions suggests that the chamber remained fairly deep. Most of the vapor loss from the 1846–47 dacite is likely to have taken place during prolonged sluggish ascent of the magma toward the surface. The narrative evidence suggests that lava effusions continued for several months and perhaps sporadically for a few years.

In experiments with comparable dacites, under conditions outside the stability field of amphibole, Rutherford and Devine (1988) found that hornblende developed Fe-oxide-rich reaction rims "in as little as 12 hours", probably by diffusive loss of hydrogen. More recent experiments by M. Rutherford (written commun. 1991), using (Mount St. Helens 18 May 1980) dacite with a glass composition (71$\pm$2% SiO_2) and phase assemblage identical to that of Quizapu dacite (Table 5), indicate that at 860°–870° C (Fig. 16) hornblende would be unstable in H_2O-saturated melt at any pressure

lower than 1250 bars. At this pressure and temperature, the saturated melt contains ~4.5 wt% H_2O, which is therefore the apparent minimum amount necessary for such melts to sustain stable amphibole. The data thus suggest that ascent of a H_2O-saturated, progressively degassing, 860° C dacite magma to any depth shallower than ~4 km should have destabilized its amphibole. The F content of 0.28–0.50 wt% in Quizapu hornblendes could have promoted stability to still shallower levels, but this effect is unlikely to be large. In experiments at slightly lower pressure (900 bars), Rutherford found that the same H_2O-saturated dacite magma at 860° C developed 12 μm rims in 4 days and 20 μm rims in 10 days, but decompression experiments show that such rims might still be undetectable after an ascent faster than 6 days. Because opaque rims did not develop on hornblendes in fully glassy parts of the 1846–47 lavas, the time interval for loss of the *final* ~4.5 wt% H_2O, during syneruptive ascent but prior to effusive quenching, might thus have been on the order of a few days. The dike that initially led the way to the surface could have depressurized and completely degassed much more slowly; if so, and if the earliest lobe of 1846–47 lava can be identified, its amphiboles should exhibit well-developed reaction rims. Some of the magmatic degassing, with attendant deuterium-depletion of the melt and consequent D/H readjustment of the (unrimmed) amphiboles, however, could have taken place at depth rather than in the conduit, possibly on a time scale of weeks or months, in response to modest depressurization of the saturated roof-zone of the chamber during the protracted magma withdrawal feeding the effusive eruption. To be more certain about the timing of degassing, we need to know more about the relative rates of hydrogen-isotope reequilibration and opaque-rim growth in magmatic hornblende.

In contrast to the protracted effusive process of 1846–47, essentially identical dacite magma broke out abruptly in 1932, depressurized, degassed, vesiculated, and quenched to plinian pumice within seconds, and accordingly retains pristine unrimmed amphibole. The wide range of δD values for 1932 hornblendes (Fig. 18) therefore suggests that pre-eruptive and non-uniform degassing had affected parts of the magma reservoir – possibly in response to the loss of 5 km^3 of magma in 1846–47 and possibly related additionally to the phreatic and mafic strombolian activity of 1907–31. Supporting the likelihood that the nonuniform lowering of δD for 1932 magma had been pre-eruptive rather than syneruptive is the lack of any relation between δD_{hb} values and eruptive sequence. Rhyodacite pumice blocks emplaced early and late in the plinian phase both yield δD_{hb} values of about −60, and the heaviest values determined (−37 and −27) are for dacites erupted early as pumice and late as a poorly vesicular breadcrust bomb.

The apparent absence among the 1932 ejecta of massive vitrophyre fragments comparable to obsidian chips studied elsewhere by Taylor et al. (1983) and Newman et al. (1988) may signify that the 1932 dacite breakout was *not* preceded by upward penetration of a dacite dike or shallow intrusion prior to vesiculation and fragmentation. Instead, the dacite magma reservoir may have breached laterally into the adjacent conduit of an independent mafic eruption already in progress. Soon after the connection sealed at the end of the plinian period, the andesite-basalt eruptive event resumed, essentially free of dacite, on the small scale typical of numerous 1907–31 events.

There is no evidence that the dacite magma had been exhausted, nor is there a persuasive basis for assuming that the post-plinian mafic magma had contiguously underlain the dacite in the same "chamber". The terminal scoria shows little or no contamination by dacite, and at no stage was cumulate mush (cf. Druitt and Bacon 1989) withdrawn from deep parts of the reservoir. The dacite magma body may not even directly underlie the Quizapu vent, as this vent has provided the outlet for dacite-free basaltic-to-andesitic eruptions both before and after the plinian event. The historically unique phreatic activity that began at nearby Descabezado Grande only two weeks after the Quizapu event of 1932 suggests the likelihood of magmatic dike emplacement beneath a larger area. Some of the phenocryst-rich andesitic initial scoria may already have been stored shallowly beneath Quizapu before the 1932 outbreak, but the basaltic terminal scoria is likely to represent a new batch arriving from the deep crust.

Consideration of the historic activity at Quizapu raises several additional points of general volcanological interest.

(1) A large effusion of silicic lava need not signify that a magma reservoir has degassed sufficiently that near-future explosive eruptions can be ruled out. The Llao Rock-Cleetwood-climactic eruptive sequence at Mount Mazama (two lava flows followed by a caldera-forming pyroclastic eruption; Bacon 1983; Bacon and Druitt 1989) illustrates this point still more dramatically.

(2) Magma discharge rate is certainly influenced by conduit dimensions, but there need be no simple relationship; the influence of non-explosive degassing history on viscosity during gradual decompression (Eichelberger et al. 1986) can impose a stronger control. At Quizapu, similar volumes of otherwise identical dacite magma erupted through approximately the same conduit twice, in 1932 at $>10^8$ kg/s and in 1846–47 at a rate at least two orders of magnitude slower. The geometry of the 1846–47 effusive vent is not well established, but the section exposed on the crater wall is ~100 m wide (Fig. 5) and, interpreting the descriptions of early visitors (Domeyko 1903; Vogel 1913, 1920), the vent seems likely to have been a N-to-NE-trending fissure as long as ~1 km. If so, its cross-sectional area may actually have been larger than that of the nearly circular plinian vent (r ~ 150 m) of 1932. At unexposed deeper levels, there is no basis for assuming the dacite conduits of 1846–47 and 1932 were very different.

(3) Discharge of fairly large volumes of magma can take place without obvious surface subsidence. The 5 km^3 (1846–47) and 4 km^3 (1932) magma volumes estimated for Quizapu are thought to be conservative val-

ues. The Quizapu subsystem may be a component of a larger, more complex, magma-storage system underlying much of the Azul-Descabezado cluster (Fig. 2); this could facilitate compensatory magma transfer beneath a broad area. The strength of the immediate basement, consisting of the massive Invernada pluton could also have been a factor in preventing subsidence. In any event, even the combined total of 9 km^3 falls near the empirical lower threshold for caldera-forming eruptions. For example, Santa María (Guatemala) discharged as much as 8.5 km^3 of dacite magma in 1902 (Williams and Self 1983) without collapse; and the ~ 12 km^3 zoned eruption at Novarupta (Alaska) in 1912 was only partly compensated by ~ 5 km^3 of collapse atop nearby Mount Katmai (Hildreth 1987, 1991).

(4) Inflections on log Thickness vs $Area^{1/2}$ plots of fallout distribution (Fig. 9) need have nothing to do with contributions of coignimbrite ash. Such inflections may be common for purely plinian fallout, and they probably reflect a discontinuity in transport, settling, and particle-aggregation properties between ash coarser and finer than ~ 0.25 mm. For the total grain-size population of many strictly plinian eruptions, >80 wt% may be finer than 1 mm and >50 wt% finer than 0.1 mm.

(5) Open-crater activity like that at Quizapu after 1907, characterized by alternating phreatic, magmatic, and phreatomagmatic eruptions, offers a straightforward mechanism for bringing meteoric water and hydrothermally altered conduit rocks into direct contact with magma. Permeable altered breccias of active and older conduits would provide H_2O-rich assimilants whenever they were stoped into the reservoir or whenever magma re-intruded upward. Long-lived open craters could thus permit direct access to the magma of ^{10}Be and other trace contaminants. Phenocrysts separated from 1932 Quizapu dacite contain significant amounts of ^{10}Be (M. C. Monaghan, work in progress); only detailed work can distinguish whether this ^{10}Be is slab-derived or whether it entered the magma from above.

(6) The ratios Ba/La, Ba/Ta, La/Yb, Zr/Hf, Zr/Y, Zr/Rb, and $^{87}Sr/^{86}Sr$ all exhibit systematic zoning (Figs. 13, 17) in products of the 18-hour plinian eruption of 1932. This indicates that all these ratios can be modified by crustal processes within crustal magma reservoirs and that none necessarily reflects a "mantle signature".

(7) Zoned eruptions need not entirely represent zoning in a magma chamber. Although any chamber containing evolved magma is likely to be zoned, not all newly ascending mafic batches have to be intercepted by such chambers. The subordinate rhyodacite of 1932 probably did come from a small zoned cap or apophysis at the chamber roof, and the "brown band" (Fig. 7) could well reflect a brief "draw-up" (Blake and Ivey 1986) of subjacent andesitic or mixed interface magma from beneath the main dacite layer during the interval of peak discharge rate. The pre- and post-plinian mafic magmas, however, are unlikely to have occupied the same chamber as the dacite. The low-temperature (Fig. 16), phenocryst-rich (andesitic) initial scoriae may represent magma that had been stored independently since the episode of mafic strombolian activity at Quizapu in the late 1920's. The post-plinian basaltic scoria probably represents a 1932 magma batch that mostly bypassed the nearby silicic magma reservoir.

(8) The induction of eruptions from silicic magma chambers by new arrivals of mafic magma can take many forms. "Triggering" is too hyperbolic a term because it implies that the response is rapid. "Replenishment" is commonly inappropriate because it implies replacement of what has already been withdrawn. The 1846 outbreak may well have been a delayed response to direct injection of the dacite chamber by the mafic magma now represented by abundant chilled inclusions dispersed in the lava flows. Their wide convective dispersal clearly took time, however, and the ensuing protracted effusions don't appear to reflect any dramatic vesiculation-induced overpressure. The 1932 plinian outbreak, on the other hand, appears to represent an accident of proximity rather than a response to some event in the dacite magma reservoir. A vigorous phreatomagmatic episode, involving andesitic magma ascending along an established conduit that had been intermittently active since 1907, may have mined down sufficiently to shatter some structural septum, permitting abrupt decompression of the adjacent dacite magma reservoir. The post-plinian basalt and the phreatic eruptions 7 km north suggest, however, that there were also new mafic injections in 1932. Whether one or more mafic dikes actually intruded the dacite magma body is unknown.

The magma storage system

As a flank vent of Cerro Azul, Quizapu lies near the southern end of a complex volcanic field, elongate N-S and dominated by the two young stratocones (Fig. 2). Although both main cones erupted mafic and intermediate magmas until at least middle Holocene time, the youngest (post-Neoglacial) central eruption of each produced rhyodacite lava ($\sim 69\%$ SiO_2). Additionally, seven rhyodacite lava flows ($\sim 71\%$ SiO_2) are arranged around the northern base of the larger cone, Descabezado Grande (Fig. 2); one flow is very young (<2000 ka?) and the other six are lightly ice-scoured, probably of latest Pleistocene (or Neoglacial?) age. Young mafic cinder cones are confined to the periphery of the field (Fig. 2), suggesting that any late Holocene magmas ascending beneath the focal region have consistently been intercepted by a shallow reservoir of evolved low-density magma. The distance from Quizapu to the northerly line of rhyodacites is 7–8 km, similar to the spread of preclimactic rhyodacite vents on the rim of Crater Lake caldera (Mount Mazama, Oregon; Bacon 1983).

The following observations, however, seem to weigh against the existence of a large, integrated, potentially caldera-forming, reservoir of rhyodacite magma beneath the Azul-Descabezado cluster in the recent past. (1) The young rhyodacites contain contrasting pheno-

cryst assemblages; one has biotite, Quizapu and two others have hornblende, but most have pyroxenes and lack hydrous phases. (2) There is no systematic age progression toward more evolved compositions among these rhyodacites. (3) Each large eruption of Quizapu was accompanied by an increment of andesitic magma, suggesting that the silicic magma layer was not necessarily very thick.

There are nonetheless so many resemblances between the Azul-Descabezado and Mount Mazama systems that we are now undertaking a broader investigation of the volcanic field, partly in order to evaluate more closely whether a large reservoir of silicic magma may recently have been coalescing there. Indeed, detailed consideration of preclimactic Mount Mazama (Bacon 1983, 1986; Bacon and Druitt 1988; Druitt and Bacon 1989) suggests that the three objections just raised against an integrated silicic magma reservoir may not be critical. The resemblances include: (1) Distributed emplacement of several rhyodacites, their vent locations not obviously controlled by regional tectonic patterns, around a cluster of previously mafic-to-intermediate stratocones; (2) comparable dimensions of the areas spanned by young rhyodacite vents in the two systems; (3) appearance of H_2O-rich hornblende-bearing rhyodacite on segments of volcanic fronts where amphibole (and biotite) are otherwise scarce; (4) exclusion of mafic cinder cones from the focus; (5) silicic-mafic mixed eruptions at the periphery; (6) a modest plinian eruption ($>2\,km^3$ DRE, Llao Rock pumice) of hornblende rhyodacite, without caldera collapse; (7) extrusion of a large lava flow of hornblende-rich rhyodacite containing abundant well-dispersed mafic magmatic inclusions (Llao Rock, emplaced 100–200 years before the climactic, caldera-forming eruption); and (8) effusion of another lava flow (Cleetwood) immediately preceding climactic plinian eruption of compositionally identical magma.

Bacon (1983) suggested that the Llao Rock and Cleetwood episodes could have unloaded the top of the magma chamber sufficiently to initiate the sustained vesiculation at depth that led ultimately to the climactic plinian outbreak. If 1846–47 were equivalent to the Llao Rock episode and 1932 to the climactic eruption, then Quizapu may be quiet for a long time to come. But it seems equally possible that both silicic eruptions of Quizapu are analogous to the Llao Rock episode and were thus preliminary, preclimactic leaks from a much larger reservoir.

Acknowledgements. The project was funded in part by National Science Foundation grant EAR 80-18354 and by a G. K. Gilbert Fellowship from the U.S. Geological Survey. We thank Warren Sharp, Anita Grunder, John Dilles, Dan Tormey, Judy Fierstein, Gail Mahood, and Michael Ort for contributions to the fieldwork over the course of many seasons. Teresa Iriarte, Leopoldo López, Francisco Munizaga, Mario Vergara, Alfredo Lahsen, and Manuel Briones provided important logistical assistance. Hugo Moreno has shared his expertise in Andean volcanology on numerous stimulating occasions. Nancy Blair, Ellen White, and the USGS Library staff helped locate many of the older reports cited. Judy Fierstein did many of the point counts, expertly drafted the diagrams, and she and Manuel Nathenson helped with the volume calculations. Charlie Bacon made numerous insightful suggestions and helped with the Fe-Ti-oxide temperature calculations. Mac Rutherford and Marie Johnson commented on the problems of Quizapu hornblende stability and generously provided soon-to-be-published experimental constraints on H_2O contents and decompression rates of such hornblende-dacite magmas. We are grateful to Doug White, Cathy Janik, and Lanny Adami for D/H determinations, to Lew Calk and Lora Stevens for help with the microprobe work, to Peggy Bruggman, Bi-Shia King, Louis Schwarz, and Joe Taggart for skilled analytical support, and to Betty Johnson and Christine Kelley for manuscript preparation. Helpful reviews by Bacon, Fierstein, Mahood, Wendell Duffield, Yukio Hayakawa, Mauro Rosi, and Andrei Sarna-Wojcicki improved the manuscript in form and substance.

References

Andersen DJ, Lindsley DH (1988) Internally consistent solution models for Fe-Mg-Mn-Ti oxides: Fe-Ti oxides. Am Mineral 73:714–726

Bacon CR (1983) Eruptive history of Mount Mazama and Crater Lake caldera, Cascade Range, USA. J Volcanol Geotherm Res 18:57–115

Bacon CR (1986) Magmatic inclusions in silicic and intermediate volcanic rocks. J Geophys Res 91:6091–6112

Bacon CR, Druitt TH (1988) Compositional evolution of the zoned calcalkaline magma chamber of Mount Mazama, Crater Lake, Oregon. Contrib Mineral Petrol 98:224–256

Bacon CR, Hirschmann MM (1988) Mg/Mn partitioning as a test for equilibrium between coexisting Fe-Ti oxides. Am Mineral 73:57–61

Bacon CR, Adami LH, Lanphere MA (1989) Direct evidence for the origin of low-^{18}O silicic magmas: Quenched samples of a magma chamber's partially fused granitoid walls, Crater Lake, Oregon. Earth Planet Sci Lett 96:199–208

Bacon CR, Newman S, Stolper EM (1988) Preeruptive volatile content, climactic eruption of Mount Mazama, Crater Lake, Oregon. Geol Soc Am Abst Prog 20/7:A248

Blake S, Ivey GN (1986) Magma mixing and the dynamics of withdrawal from stratified reservoirs. J Volcanol Geotherm Res 27:153–178

Bobillier C (1932) La erupción del Volcán Quizapu en abril de 1932. Bol Serv Sismol Univ Chile 22:33–39

Bobillier C (1934) Erupciones volcánicas en Chile. Bull Volcanol 23–26:135–138. [Author's name incorrectly given as Mr. Robillier]

Brazier S, Sparks RSJ, Carey SN, Sigurdsson H, Westgate JA (1983) Bimodal grain size distribution and secondary thickening in air-fall ash layers. Nature 301:115–119

Bruggen J (1933) Der Aschen- und Bimsstein-Ausbruch des Vulkans Quizapu in der chilenischen Kordillere. Z Vulkanol 15:100–104

Bruggen J (1950) Fundamentos de la Geología de Chile. Instituto Geográfico Militar, Santiago, 374 p

Bustos Navarrete J (1932) Die letzte vulkanische Krise. Der Ausbruch des Quizapu im April dieses Jahres. Andina (Zeitschrift für Naturfreunde und Wanderer, Mitteilungen der Sektion Chile) 10/2:24–26

Carey SN, Sigurdsson H (1982) Influence of particle aggregation on deposition of distal tephra from the May 18, 1980, eruption of Mount St Helens volcano. J Geophys Res 87:7061–7072

Carey S, Sigurdsson H (1987) Temporal variations in column height and magma discharge rate during the 79 A.D. eruption of Vesuvius. Geol Soc Am Bull 99:303–314

Carey S, Sigurdsson H (1989) The intensity of plinian eruptions. Bull Volcanol 51:28–40

Carey S, Sparks RSJ (1986) Quantitative models of the fallout and dispersal of tephra from volcanic eruption columns. Bull Volcanol 48:109–125

Craig H (1961) Isotopic variations in meteoric waters. Science 133:1702–1703

Dartayet M (1932) Observacíon de la lluvia de cenizas del 11 de abril de 1932 en La Plata. Rev Astron (Buenos Aires) 4:183–187

Dobson PF, Epstein S, Stolper EM (1989) Hydrogen isotope fractionation between coexisting vapor and silicate glasses and melts at low pressure. Geochim Cosmochim Acta 53:2723–2730

Domeyko I (1903) Jeolójia, vol 5. Imprenta Cervantes, Santiago

Drake RE (1976) Chronology of Cenozoic igneous and tectonic events in the central Chilean Andes - latitudes 35°30′ to 36° S. J Volcanol Geotherm Res 1:265–284

Druitt TH, Bacon CR (1989) Petrology of the zoned calcalkaline magma chamber of Mount Mazama, Crater Lake, Oregon. Contrib Mineral Petrol 101:245–259

Eichelberger JC, Carrigan CR, Westrich HR, Price RH (1986) Non-explosive silicic volcanism. Nature 323:598–602

Fierstein J, Hildreth W (1991) The plinian eruptions of 1912 at Novarupta, Katmai National Park, Alaska. Bull Volcanol (in review)

Fierstein J, Nathenson M (1991) Another look at the calculation of fallout tephra volumes. Bull Volcanol (in press)

Friedlaender J (1933) Der grosse Ausbruch in der chilenisch-argentinischen Kordillere im April 1932. Z Vulkanol 15:116–123

Frost BR, Lindsley DH, Andersen DJ (1988) Fe-Ti oxide-silicate equilibria: Assemblages with fayalitic olivine. Am Mineral 73:727–740

Fuenzalida H (1941) Distribución de los volcanes del grupo de los Descabezados. Bol Museo Nac Hist Nat (Santiago) 19:19–30

Fuenzalida H (1942) El Volcán Descabezado Grande. Bol Museo Nac Hist Nat (Santiago) 20:35–50

Fuenzalida H (1943) El Cerro Azul y el Volcán Quizapu. Bol Museo Nac Hist Nat (Santiago) 21:37–53

Godoy P (1984) Geología del Grupo Volcánico Descabezado Grande - Los Hornitos. Taller de Titulo II, GL-698, Univ Chile (Santiago), Depto Geol Geofis, 125 p

González Ferrán O, Vergara M (1962) Reconocimiento geológico de la Cordillera de los Andes entre los paralelos 35° y 38° latitud sur. Univ Chile, Inst Geol, Publ 24, 121 p

Grunder AL (1987) Low $\delta^{18}O$ silicic volcanic rocks at the Calabozos caldera complex, southern Andes. Contrib Mineral Petrol 95:71–81

Grunder AL, Mahood GA (1988) Physical and chemical models of zoned silicic magmas: The Loma Seca Tuff and Calabozos caldera, Southern Andes. J Petrology 29:831–867

Hildreth W (1987) New perspectives on the eruption of 1912 in the Valley of Ten Thousand Smokes, Katmai National Park, Alaska. Bull Volcanol 49:680–693

Hildreth W (1991) Timing of caldera collapse at Mount Katmai in response to magma withdrawal toward Novarupta. Geophys Res Lett, in press

Hildreth W, Moorbath S (1988) Crustal contributions to arc magmatism in the Andes of central Chile. Contrib Mineral Petrol 98:455–489

Hildreth W, Grunder AL, Drake RE (1984) The Loma Seca Tuff and the Calabozos caldera: a major ash-flow and caldera complex in the southern Andes of central Chile. Geol Soc Am Bull 95:45–54

Huebner JS, Sato M (1970) The oxygen fugacity-temperature relationships of manganese oxide and nickel oxide buffers. Am Mineral 55:934–952

Jones HS (1932) The Andean eruption and sunset and sunrise glows in South Africa. Nature 130:279

Kittl E (1933) Estudio sobre los fenómenos volvánicos y material caído durante la erupción del grupo del "Descabezado" en el mes be abril de 1932. Anal Museo Nac Hist Nat (Buenos Aires) 37:321–364

Kobayashi T, Hayakawa Y, Aramaki S (1983) Thickness and grain-size distribution of the Osumi pumice fall deposit from the Aira caldera. Bull Volcanol Soc Japan 28:129–139

Kreutz S, Jurek M (1932) Cendres volcaniques tombées en Avril 1932 à Buenos Aires. Polskiego Towarzystwo Geologiczna Rocznik (Krakow) 8:316–330

Larsson W (1937) Vulkanische Asche vom Ausbruch des chilenischen Vulkans Quizapu (1932) in Argentina gesammelt. Geol Inst Upsala Bull 26:27–52

Lindsley DH (1983) Pyroxene thermometry. Amer Mineral 68:477–493

Lirer L, Pescatore T, Booth B, Walker GPL (1973) Two plinian pumice-fall deposits from Somma-Vesuvius, Italy. Geol Soc Am Bull 84:759–772

Lunkenheimer F (1932) La erupción del Quizapu en abril de 1932. Rev Astron (Buenos Aires) 4:173–182

Maass A (1932) 14 Tage in der Kordillere von Talca, der Zone der tätigen Vulkane. Andina (Zeitschrift für Naturfreunde und Wanderer, Mitteilungen der Sektion Chile) 10/2:27–37

Merzbacher C, Eggler DH (1984) A magmatic geohygrometer: applications to Mount St Helens and other dacitic magmas. Geology 12:587–590

Moreno Roa H (1982) Descabezado Grande Volcano, Central Chile. SEAN Bulletin (Smithsonian Inst) 7/3:17

Newman S, Epstein S, Stolper E (1988) Water, carbon dioxide, and hydrogen isotopes in glasses from the ca. 1340 A.D. eruption of the Mono Craters, California: Constraints on degassing phenomena and initial volatile content. J Volcanol Geotherm Res 35:75–96

Pyle DM (1989) The thickness, volume, and grainsize of tephra fall deposits. Bull Volcanol 51:1–15

Reck H (1933) Der Ausbruch des Quizapu vom 10–11 April 1932 und seine Folgen. Naturwissenschaften 21:617–624

Riso Patrón L (1917) Las exploraciones del señor Mauricio Vogel en las cordilleras del Centro. Rev Chilena d Hist Geogr 23:371–381

Rutherford MJ, Devine JD (1988) The May 18, 1980, eruption of Mount St Helens, 3. Stability and chemistry of amphibole in the magma chamber. J Geophys Res 93:11949–11959

Sarna-Wojcicki AM, Shipley S, Waitt R Jr, Dzurisin D, Wood S (1981) Areal distribution, thickness, mass, volume, and grainsize of airfall ash from the six major eruptions of 1980. US Geol Surv Prof Pap 1250:577–600

Sigurdsson H, Carey S, Cornell W, Pescatore T (1985) The eruption of Vesuvius in 79 A.D. Nat Geogr Res 1:332–387

Simkin T, Siebert L, McClelland L, Bridge D, Newhall C, Latter JH (1981) Volcanoes of the World. Smithsonian Inst, Washington, 233 p

Sorem RK (1982) Volcanic ash clusters: Tephra rafts and scavengers. J Volcanol Geotherm Res 13:63–71

Sparks RSJ (1986) The dimensions and dynamics of volcanic eruption columns. Bull Volcanol 48:3–15

Stormer JC (1983) The effects of recalculation on estimates of temperature and oxygen fugacity from analyses of multicomponent iron-titanium oxides. Am Mineral 68:586–594

Suzuoki T, Epstein S (1976) Hydrogen isotope fractionation between OH-bearing minerals and water. Geochim Cosmochim Acta 40:1229–1240

Taylor HP Jr, Sheppard SMF (1986) Igneous rocks: I. Processes of isotopic fractionation and isotope systematics. In: Valley JW, Taylor HP Jr, O'Neil JR (eds) Stable isotopes in high temperature geological processes. Rev Mineral 16:227–271

Taylor BE, Eichelberger JC, Westrich HR (1983) Hydrogen isotopic evidence of rhyolitic magma degassing during shallow intrusion and eruption. Nature 306:541–545

Vogel M (1913) Reisebilder aus den Hochkordilleren der Provinz Talca, speziell aus der Zone des tätigen Vulkans. Verh Dtsch Wissen Vereins zu Santiago de Chile 6:263–313

Vogel M (1920) Reisebilder aus den Hochkordilleren der Provinz Talca: Ergebnisse meiner dritten Reise 1916. Verh Dtsch Wissen Vereins zu Santiago de Chile 6:454–480

Vogel M (1933) Bericht über vulkanische Vorgänge in Mittelchile und den angrenzenden Provinzen Argentiniens, besonders über die Vulkane Descabezado Grande und Cerro Azul (Quizapu). Z Vulkanol 15:105–115

Walker GPL (1973) Explosive volcanic eruptions – a new classification scheme. Geol Rundsch 62:431–446

Walker GPL (1980) The Taupo pumice: Product of the most powerful known (ultraplinian) eruption? J Volcanol Geotherm Res 8:69–94

Walker GPL (1981a) Plinian eruptions and their products. Bull Volcanol 44:223–240

Walker GPL (1981b) The Waimihia and Hatepe plinian deposits from the rhyolitic Taupo volcanic centre. NZ J Geol Geophys 24:305–324

Walker GPL, Croasdale R (1971) Two plinian-type eruptions in the Azores. J Geol Soc London 127:17–55

Wilson L, Walker GPL (1987) Explosive volcanic eruptions – VI. Ejecta dispersal in plinian eruptions: the control of eruption conditions and atmospheric properties. Geophys J R Astron Soc 89:657–679

Wilson L, Sparks RSJ, Walker GPL (1980) Explosive volcanic eruptions – IV. The control of magma properties and conduit geometry on eruption column behavior. Geophys J R Astron Soc 63:117–148

Williams S, Self S (1983) The October 1902 plinian eruption of Santa María volcano, Guatemala. J Volcanol Geotherm Res 16:33–56

Editorial responsibility: B. F. Houghton